# Copper Oxide Nanoparticles Loaded Chitosan Films for Adsorption of Azo Dyes



**By**

**Hafsa Anam**

**School of Chemical and Materials Engineering (SCME)**

**National University of Sciences and Technology (NUST)**

**2019**

# Copper Oxide NanoParticles Loaded Chitosan Films for Adsorption of Azo Dyes

By: Hafsa Anam

Reg No:NUST201500000119214

**This work is submitted as a MS thesis in partial fulfillment of the requirement for the degree in of MS in Nanosciences and Engineering**

**Supervisor name: Dr. Zakir Hussain**

**School of Chemical and Materials Engineering (SCME)**

**National University of Sciences and Technology (NUST), Year 2019**

*Dedicated to my loving parents and brothers*

# Acknowledgment

First of all I am highly grateful to **Allah Almighty**, who provided me with knowledge and opportunity that I have successfully crossed another milestone of my academic carrier and completed my thesis well in time with success.

I owe special thanks to my supervisor **Prof.Dr Zakir Hussain** and deepest gratitude to my Family who always prayed for me and taught me that even the largest task can be accomplished with patience and hard work. My special thanks to all of my seniors and friends for their possible assistance during my research work.

_____

**Hafsa Anam**

# Abstract

Textile effluents contain variety of chemicals that have complex chemical composition and due to their stable nature they are difficult to be treated. There are different techniques for dye removal which includes chemical, physical and biological. Amongst these nano sized metal oxide nanoparticles and chitosan based porous films as adsorbents attracted much attention due to its low cost. Present study aims at using Neem leaves (*Azadirachta indica)* leaf extract for the preparation of NPs.In this work, a novel adsorptive membranes of chitosan/poly ethylene glycol (CH/PEG/CuO) nano composites were prepared:wherein Chitosan provides functional groups ($-NH_2$) while PEG provides strength. Copper oxide(CuO) NPs were incorporated to determine its effect on Chitosan/PEG blend films. It was found that the two polymers were miscible in the blends of Chitosan PEG and CuO NPs. By adjusting the polymer concentration in solution, a variety of CH/PEG/CuO nano composite films with surface pore size in the range of ~120nm-250 nm analyzed from SEM were prepared. Moreover, PEG was added as a solution modifier. The fabricated nano composites were characterized using  SEM

, FTIR , (UV-Vis) spectroscopy and XRD.  Batch experiments were conducted at varying parameters like  dye concentration, nano adsorbent mass  and effect of contact time to compare  adsorptive efficiency of nano adsorbents. Results indicated that the methyl orange removal was more in comparison with Methylene Blue. Optimal removal of  96% was obtained for azo dyes. Contact time and kinetics of adsorption confirmed that the process could be explained by second order kinetics. This study concludes that biosynthesis procedure applied; offer simple, ecofriendly and cost effective method for nano adsorbents synthesis .

# Table of Contents

**Chapter3: Results and Discussion**

# List of Figures

# List of Tables

# Abbreviations

| NPs | Nano particles |
|------|----------------|
| NLE | Neem leaf extract |
| GNP | Gross National Product |
| WWF | World Wide Fund |
| FTIR | Fourier Transform Infrared Spectrometer |
| CH | Chitosan |
| PEG | poly ethylene glycol |
| NC | Nano composite |

# CHAPTER 1

# INTRODUCTION

## 1.1 Introduction

Earth comprises about 3% of freshwater hence its conservation is important for saving planet. [1]. With the industrial revolution which started in late 18th and 19th century, natural resources were exploited for more production and material output. Environmental issues got recognition in later half of the 20th century [2].

Increase demands for textile products, leading to increased number of industries overall due to which its waste water load have been increasing continuously[3] [4]. Around 2,000 million gallons of waste effluent is being poured into water bodies every day [5]. 80% of textile waste is generated by different industries like sugar, textile and cement [6].

Strong color is integral part of tanneries waste. The dye stuffs are highly complex structured compounds and they are very difficult to decompose biologically [7] [8].
For processing of about 1kg of textile effluent 100 L of water is used. All the dye molecules donot bind to the fabric during dying process it was estimated around 280,000 tons of tanneries waste being discharged openly annually [9].

## 1.2 Types of dyes

Dyes are unsaturated organic molecules, used to give color to a material[10] . Dyes are classified on number of ways including color, trade name, chemical compositon and chemical structure.Chemical composition relates to the major chromophore present in dye [11]. In dying process, different dyes are used such as Anionic,cationic (basic dyes) ,non ionic depending on the charge present on dye molecule. [12]. Disperse Azo,Diazo and metal complex dyes. [13]. More than 100,000 commercial  dyes  than are available with over 700,000 tons produced annually [14]. Major classes of synthetically produced  dyes are Azo

and Anthraquinonone they represent 90% of all organic dyes altogether. Important thing to note over here is that dye molecules consists of varying structure and their adsorption is directly related to chemical structure, dimensions of chains, numbering and position of functional groups and organic chains. These are among the most vital influencing factors for adsorption. [15].

Two aromatic groups are present normally in Azo groups. Az dyes are one of the most important class of industrial dyes available commercially,both in number and amount produced ,they are important because, [16]

1. They cover entire spectrum.
2. They have fair to good fastness properties.
3. There are cost-effective

Textile wastewater is quite resistant to biodegradation due to dye stuff present i.e stable and have complex chemical structure as well as resistant to heat , light and oxidative agents [17]. A very less quantity of dyes impart color in aqueous media and they can be recognized at very less amount. [18].which affects aesthetically and also reduces light penetration which is an important factor for photosynthesis due to thin layer formed on the upper surface hence it directly affects aquatic flora and fauna moreover in addition to being toxic ,dye stuff contains harsh chemicals that are mutagenic to living organisms [18].

Basic dye like Methylene blue is considered to be one of the most toxic substance it can cause breathing problems on nausea vomiting etc. can even cause problems regarding eyes which ultimately leads to permanent eye injury some types of dyes also can cause allergy dermatitis skin allergies, and even cancer in living organisms. Therefore their removal is must before their discharge [19].

Since dyes have very low biodegradability, the modern waste treatment methods are not effective in remediation of dyes there are different techniques for dye removal. Every method has its certain merits and lmitations commonly they are categorized in three; physical,chemical,biological. [20].

## 1.3 Literature survey

In a research study reactive black 5 (RB5) dye was degraded by combined biological and photo catalytic (UV/TiO2) method. 60% chemical oxygen demand removal was achieved through biological step. The use of (TiO2) for remediation of dyes is technically a practicable approach for clean up but requirement for UV light and very low yield makes its use difficult in practical remediation techniques [21].

Chemical methods like ozonation [22] for adsorption of red C1-5B dye at varying parameters . more than 90% removal was achieved by this method.

In dye removal processes fungal extracted enzymes have also been studied [23]. Decolorized cationic dye (Basic Blue 41) using horseradish peroxidase enzymes and sulfonated polymers extracted from a fungus, at different pH. Very less decolorization was observed with Horseradish peroxidase enzyme.

In another study they Attempted Congo red removal an acidic dye by using activated carbon . About 90% dyes was removed successfully for 50 mg/L and 100mg/L concentrations at pH 7 [24].

Thus common remediation techniques which require high energy, cost and also result in formation of large amount of chemical sludge. Medium-size factories can prefer physical and chemical techniques by using flocculates or coagulants due to economical concerns but they also have short life time, biological methods are quite complicated and unfortunately for the developing countries, like Pakistan these processes are still very costly to be used at large scale and they cannot be practiced by small industries to treat large volume of wastewater . This situation emphasized need to develop alternative novel methods which are more cost effective and environment friendly [25].

## 1.4 Nano particles as sorbents

Clusters of atoms which range in size from 1-100 nm are called as nano particles consist sof two categories like organic NPs e.g inorganic and organic which include noble metals like silver and gold as well as NPs made of semi conductors such as $TiO_2$ and $ZnO_2$ however metallic NPs e.g. silver, gold, palladium, iron and copper etc hold quite remarkable properties in various fields; with the advancement in nanotechnology it provides us with alternative

routes to physical and chemical for synthesis of nano clusters. Variety of chemical methods which include Sol Gel, microwave irradiation, Sono chemical and quick precipitation method which uses harsh reducing agents and organic solvents. [26].

Nanosized NPs have received quite attention recently because of the procedure adopted for Its synthesis is cost effective compared to commercially available activated carbon.NPs have very interesting properties such as high electrical conductivity, high thermal conductivity, metallic or semi metallic behavior ,ordered structure high mechanical strength and high surface area. Due to which NPs are considered to be building blocks for next generation. Transition metals oxides are an important class of semiconductors, like copper oxide NPs because they exhibit catalytic. Photonic, electric, optical and anti bacterial properties. Although many physical and chemical methods have been extensively used to produce monocrystalline copper oxide such as micro emulsion method, but the consumption of harsh chemicals is of concern [27].

Many low cost adsorbents have been introduced including activated Carbon, by products from industrial waste, peat, zeolites and green biomass attracted special attention .The reason why biosynthesis approach was preferred over chemical routes is because plant contains natural reducing agents e.g ascorbic acid, flavonoids , reductaces ,citric acid they act as important entity for NPs synthesis. recent studies have focused merely on removing dye stuffs from waste  water system using  noble metals and their nano-particles .so synthesis of transition metal nanoparticles like copper from bio source and use of these particles as nano adsorbents for  degradation of dyes is an economic, fast, eco friendly and convenient step for textile  by products [28].

Copper NPs were synthesized chemical reduction of copper sulfate along with sodium phosphate in ethylene glycol and using PVP as capping agent. Size of NPs ranges from 30 to 65 nm by altering reaction parameters like temperature and pH [39].

Another study reported a facile green approach for Copper oxide synthesis using (*Citrus medica Linn*) juice which is quite effective and non toxic method with average particles size in 10-60nm and concentration of $2.18 \times 10^8$ [30].

Cuprous oxide (Cu$_2$O) NPs were synthesized using mild solvents such as (*Camellia sinensis*) leaves extract with Average diameter in range of 34nm [31].

In another research study they reported green synthesis of CuO NPs (*Carica Papaya*) leaves. UV Vis reveals formation of copper oxide NPs. they were rod shaped with average diameter in range of 140nm [32]

Nano crystalline CuO NPs were synthesized using brown algae (*Bifurcaria bifurcat*) in size range of 5-45nm .XRD confirms the crystalline nature of CuO NPs [33].

The adsorption process is most effective techniques been successfully applied for dye removal from textile wastewater [34].Therefore much attention has been given to the study of different types of cost effective, non toxic, and green materials as nano sorbents for the removal of dyes, which include, apple pomace [35] ,orange peel [36], leaf extract [37]  tea waste [38]  Garlic peel [39] etc.

Mostly conventional adsorbents were used in the form of powder, which makes its use cost in effective and difficult to separate out from waste water stream moreover all of adsorption experiments were conducted under bath conditions when using powdered adsorbents; Which is unsuitable for dynamic removal of dyes especially in case of flowing streams [40]To overcome such drawbacks adsorbents in the form of thin films or porous membranes have attracted intensive interests mainly due to ease of separation as well as no generation of secondary contaminants. [41] In comparison to many other commercially available polymer based membranes [42].

## 1.5 Why Chitosan is used as an adsorbent material?

Generally four factors contribute to growing need of chitosan as a most suitable adsorbent material for dye removal [43],

1. Chitosan based materials are low cost and as an adsorbent they are very cost effective due to the simplicity in processing involved.
2. High adsorption ability and higher rate of adsorption.
3. Strong affinity for number of dyes.

4. Versatility in processing leads to different forms like fibers, gels, beads, nano particles, films and membranes.

## 1.6 Chitosan

Chitosan is prepared from chitin, a naturally occurring abundant biopolymer originating [44]. Chitosan resembles cellulose structure but it has aceto amide groups at the carbon 2 position instead of OH groups and it is amino polymer (see Fig. 1). Chitosan is generally non porous, dense in powder form which is; opaque and brittle and it is also semi crystalline biodegradable polymer in nature.

Chitosan has widely been used in fields like medical devices, healthy food, packaging, food additives, waste water treatment, etc. To bind charged substances, heavy metals and ions from aqueous solutions, chitosan is mainly used as an adsorbent and flocculant. Chitosan shows strong binding capacity for variety of charged water pollutants such as humic acids and anionic acids by hydrogen bonding and electrostatic interactions. Chitosan, in alkali solutions gives negative charge and it is positively charged in acidic solutions [45].
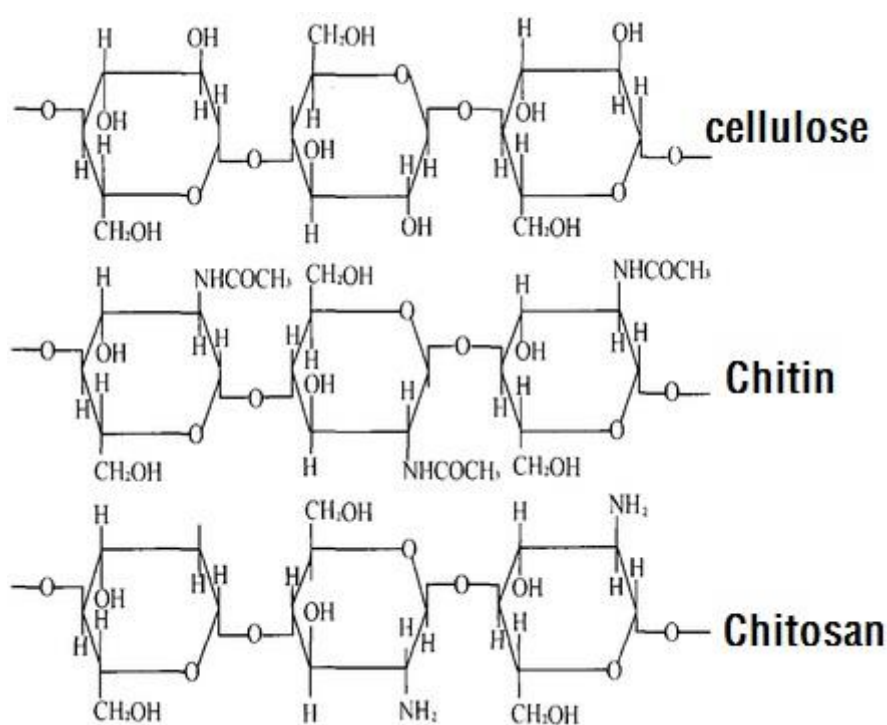


**Figure 1 Chemical structures of (1). Cellulose. (2). Chitin (3). Chitosan [57]**

Chitosan shows strong capability to capture transitional heavy metal ions because it has free amino groups, which can act as heavy metal ion chelators, by having a lone pair of electrons. The free amino groups (–NH2) can function as heavy metal ion chelators by proving a lone pair of electrons and hence chitosan shows strong ability to capture transitional metal ions. Chitosan has found to be one of the most strong heavy metal ion binders [46].

## 1.7 Chitosan based flat sheet membranes

Almost all the research studies have focused on Chitosan based membranes or flat sheet Chitosan so far. DIP) and RIP are the most commonly used methods for the preparation of chitosan membranes. In RIP, to precipitate out the membranes crosslinker must be added into coagulation solution. In DIP, Chitosan neutralization is done to form solids, base solution is added into coagulation solution. Sometimes combination of DIP and RIP methods, uses addition of basic cross linker solutions as precipitation reagent.

Chitosan flat membranes are most preferably prepared by forming a clear, viscous solution (usually (<7% m/v). first of all Chitosan is dissolved in a dilute weak acid solution (formic acid, acetic acid) for 24 hours at room temperature. Initially lower concentration of chitosan should be utilized in a solution due to formation of polyelectrolytes in an acidic solution, (NH2 $\longrightarrow$ NH3+), which significantly intensifies solution viscosity. The concentration depends highly on the molecular weight (MW) of chitosan being used. Chitosan of Low molecular weight should be used to prepare solution with high concentrations. To improve mechanical strength of Chitosan membranes, **solution casting** with bio compatible plasticizers which are highly hydrophilic, biocompatible and highly crystalline in nature e.g glycerols or polyols among them preferably poly ethylene glycol (PEG) is used; this method is the best and the membranes are still flexible due to the absence of bulky groups on chitosan polymer chains [47].

An ideal matrix for adsorptive membrane separations should hold following characteristics:

1. Low non specific adsorption.
2. High surface areas .
3. Large pore size.
4. High chemical, thermal, and mechanical stabilities
5. Sufficient functional groups on surface (e.g., hydroxyl, carboxyl, and amides) etc [60].

Chitosan is used widely for dyes and metals as a well known sorbent because Chitosan is cationic in nature it adsorbs anionic dyes and in very small amount cationic dyes [48].therefore researchers have showed great concern in its modification to enhance its properties addition of filler into polymer matrix via ex situ synthesis is a novel method for incorporating metal nano particles which helps to increase its adsorption capacity via electrostatic attractions and hydrogen bonding therefore aim of this research study was to synthesize copper oxide nano particles through green synthesis and preparation of Chitosan PEG films with incorporation of synthesized nano particles for adsorptive removal of Azo dyes.

**1.8 Objectives of the study:**

- Green synthesis of NPs through economically viable and environmental friendly method.
- Fabrication of nano composite films of chitosan, poly ethylene glycol (PEG) and CuO nanoparticles by using solution casting method.
- Application of the synthesized nano composite films as nano adsorbents for removal of selected dyes.

## 1.9 Significance of the study:

This research will be significant in devising a low cost, novel and greener synthesis of transition metal nano-particles from bio source. The development of such adsorbents can be applied for remediation techniques and in waste management system. The use of prepared bio compatible nano composite films results in reduction of waste for environmental cleanup with no generation of chemical and biological sludge.

# CHAPTER 2

## 2.1 Experimental

The present investigation is based on the green synthesis of metal nanoparticles and its application for environmental remediation. For this purpose, copper oxide nanoparticles were synthesized using Neem leaf extract. Biocompatible films were synthesized using solution casting method. A systematic characterization was performed using FTIR, XRD, DSC, Tensile testing and SEM studies.

Biosorption technique was used for the removal of environmental pollutants. UV-Visible studies were conducted for batch adsorption experiment. The sorption process was further evaluated using kinetic models and equilibrium isotherms.

## 2.2 Materials

The following table gives us the specifications of materials that were used to carry out experimentation.

| Sr.No | Materials | Manufacturer and specifications |
|-------|-----------|---------------------------------|
| 1 | Copper Sulphate pentahydrate | Sigma Aldrich Co ,USA (lab Grade) |
| 2 | Chitosan (AD>85%) | Sigma Aldrich Co ,USA (lab Grade) |
| 3 | Formic acid | Sigma Aldrich Co ,USA (lab Grade) |
| 4 | Polyethylene glycol - 6000 | Sigma Aldrich Co ,USA (lab Grade) |
| 5 | Methyl Orange | Sigma Aldrich Co ,USA (lab Grade) |
| 6 | Methylene Blue | Applichem Panreac (lab Grade) |

## 2.3 Neem Leaf Extract Preparation

**Leaf** extract of neem was prepared for the synthesis of metal nano particles. Dried neem leaves were thoroughly washed with double distilled water in order to remove any dirt or impurities. Leaves were dried and crushed with mortar and pestle, and sieved through 150 mesh size. The neem leaf powder was further added into The powder was added into 500 ml of distilled water. As extracting solvent and further boiled for an hour at 80°. The extract was further stored till further use.

## 2.4 Synthesis of Metal Nano Particles

.
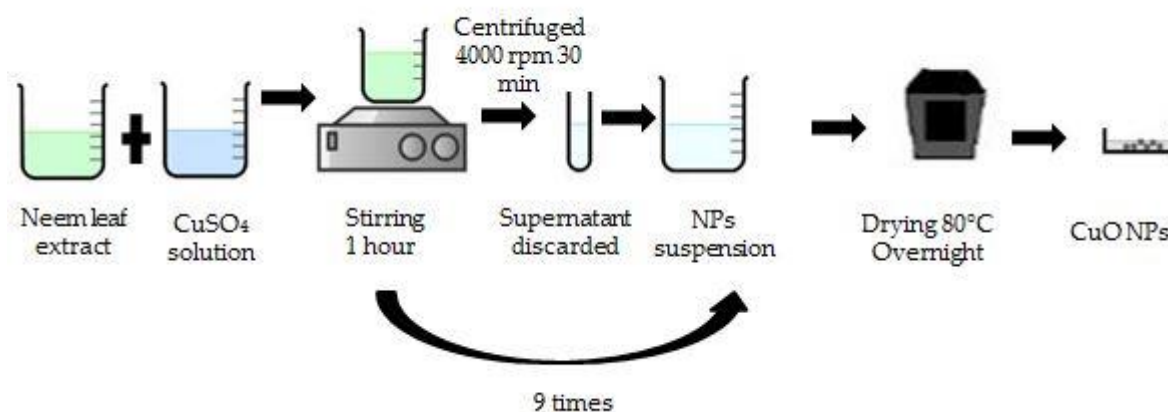


**Figure 2. General synthesis scheme of copper oxide nanoparticles**

A known volume (100 ml) of leaf extract was added to 0.5 M solution of metal salt. For synthesis of NPs .The solution was thoroughly stirred for an hour on slight heating (50-60 ℃), followed by drop wise addition of extract till the color change is indicated. Solution was further stabilized at ambient temperature, centrifuged at 4000 rpm at 4 ℃ for 30 minutes interval, multi washed, air dried and oven dried at 80° for 18 hours. The dried material was crushed with mortar pestle, sieved and stored in dessicator. The particles were of dark green brown color representing successful synthesis of CuO NPs, respectively.

For metal particles synthesis, protocol of Pattanayak and Nayak, 2013 was generally followed. The modification added to the reported method is the synthesis of Copper oxide particles from neem extract [62].

## 2.5 Preparation of Chitosan/PEG /CuO Nano composite films



- Chitosan is dissolved in formic acid
- Over night stirring

- PEG is added
- Over night stirring

- CuO NPs added
- Probe sonication for 5 Hr

- Casted in Petri dish for air drying 48 Hr
- Further dried in vacumm oven for 18 Hrs

- Dried thin film
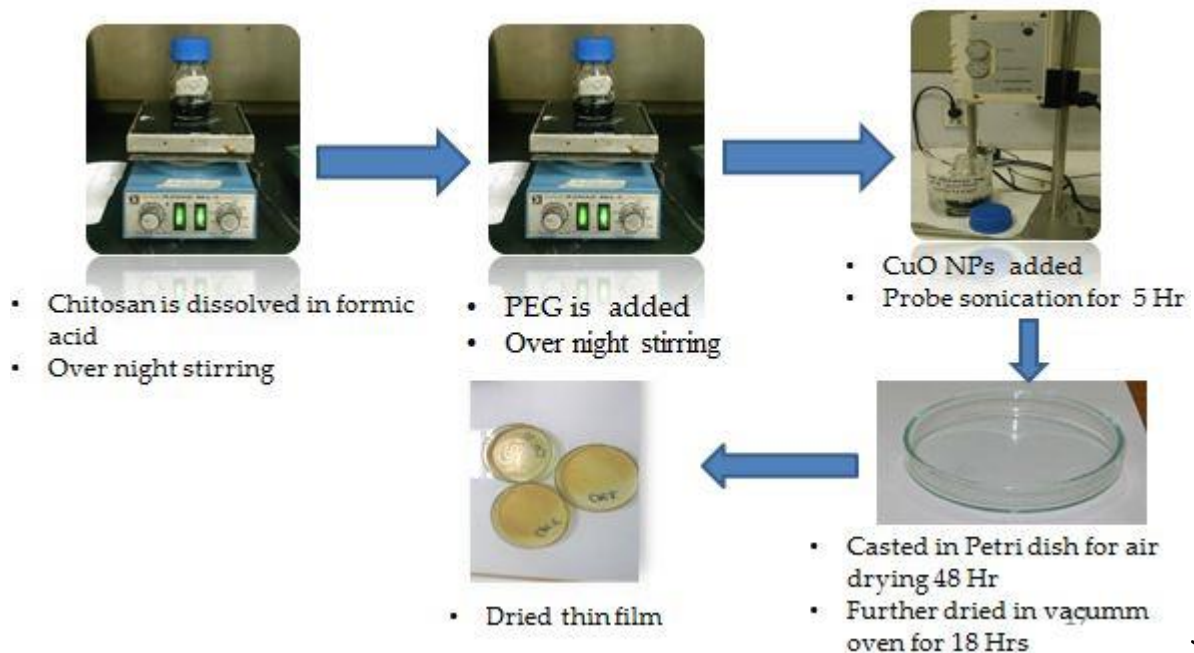
**Figure 2.1 General scheme of nano composite films preparation**

Nano composite films were prepared using solution casting and evaporation method.. 1g Chitosan was dissolved in 40ml of Analytical grade formic acid, solution was magnetically stirred for 24 hours in order to completely dissolve the polymer. After its dissolution 0.2g of poly ethylene glycol PEG (6000) was further added into the viscous solution and mechanically stirred for 24 hours. Afterwards when both polymers were completely dissolved; CuO NPs were sonicated separately for 2-3 hours and were added subsequently in to the polymer solution with different ratios of 1,5 and 10 mg respectively and further stirred for 4-6 hours using probe sonicator.

The mixture solution were then cast into Petri dishes and spread slowly to form a homogenous liquid film then left to air dry for 48hours and further washed with DI water to

remove excess formic acid .the de casted films were dried in vacuum oven at 70 °C for 18 hours. Stored in silica gel. The prepared Nanocomposite films were in green brown color see figure 2.2
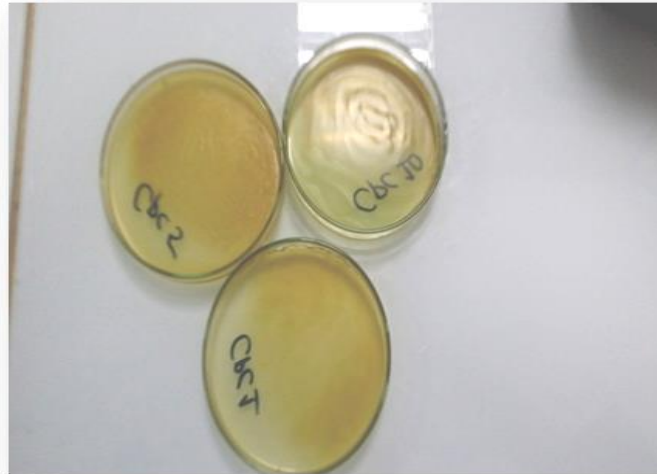


## 2.6 Characterization of CuO NPs and Chitosan/PEG films

### 2.6.1 Scanning Electron Microscope (SEM)

SEM (JEOL JSM-6490, Japan) analysis was carried out to investigate surface morphology and particle size of synthesized particles and prepared nano composite films.

### 2.6.2 Working Principle

On samples solid surface high energy ray of electron is focused. The kinetic energy of electrons dissipated their kinetic energy in samples. These signals consist significantly of backscattered and secondary electrons. Mainly Sample image is formed by backscattered electrons and secondary electrons. Backscattered electrons are more helpful in phase discrimination while secondary electrons are more significant for viewing morphology and topography of a sample.

### 2.6.2 SEM Applications

SEM analysis gives following information about sample.

- Topography: related to  surface characteristics of a sample
- Morphology: related to appearance and surface size
- Crystallography: Shows arrangement of atoms in the sample

### 2.6.3 Instrumentation

SEM consists of following parts:

- Sample stage
- Electron lenses
- Data output devices
- Detector
- Electron gun

### 2.6.4 X-RAY Diffraction (XRD)

Different types of crystalline compounds known as phases were identified and determined by means of XRD. Thus, the phases that were present in the developed CH/PEG/CuO films were studied.  Film measurements by X-ray diffraction were performed with the (STOE, Cu kα radiation ($\lambda = 0.15418$nm) for the scanning of diffraction angle between 1 to 80.

### 2.6.5 Working Principle

Every crystalline material has some regular arrangement patterns of atoms in a crystal lattice. The sample is sputtered by an x-ray beam, some part of beam is transmitted, while some part is refracted, sometimes partially diffracted and absorbed by the sample.The Bragg's Law can be defined as;
Where,
n= diffracted beam order
Lambda= x-ray beam wavelength
d= distance between plane of atoms

### 2.6.6 Instrumentation

The diffractometer of X-Ray consists of three main parts

- Sample holder
- X-ray tubes
- X-ray detector

### 2.6.7 Applications

Mostly diffraction analysis is utilized for following applications,

- To identify unknown material which is crystalline
- To measure dimensions of a unit cell
- To check  purity of  samples

### 2.6.8 Fourier transform infrared spectroscopy (FTIR)

Synthesized nano particles and Raw Neem leaves were subjected to FTIR spectrophotometer (FTIR 1500, Schimadzu Japan). The samples were pressed into KBr pellets. It is an analytical method used to obtain infrared spectrum of liquid, solid or absorption/emission of gas, or emission. The term Fourier transform refers to mathematical process where Fourier transform is required to obtain desired spectrum from raw data. It is used for qualitative and quantitative analysis of inorganic samples and organic. This method is most efficient. For detection of functional groups and identification of different chemical bonds present in sample under test.

### 2.6.9 Working principle

In FTIR analysis radiations are passed through the sample. Some radiations are transmitted while some are absorbed by the sample. FTIR spectrum is obtained On the basis of transmitted and adsorbed radiations. The resulting spectrum forms a fingerprint of sample, which is used to identify the sample. The frequency range being measured in terms of wave number, which varies from 4000-400 $cm^{-1}$.
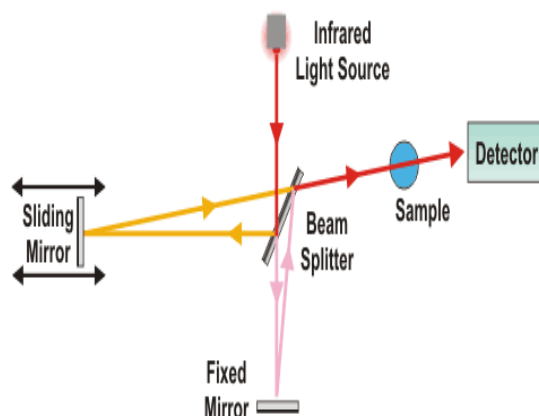
**Figure 2.3. Schematic of Fourier Transform Infrared Spectroscopy (FTIR)**

### 2.6.10 Instrumentation

FTIR spectrometer mainly consists of following:

- Sample chamber
- IR source
- Interferometer and IR detector

### 2.6.11 Applications

FTIR analysis is widely used for following applications:

- To identify unknown materials
- To determine quality of  sample
- detection of  chemical bonds present in the sample
- functional groups identification

## 2.7 Tensile Testing

Tensile properties of pure and composite films were determined films were determined using Trapezium machine manufactured by Shimadzu Corporation at speed of 1mm/minute (ASTM D822).

## 2.8 Experimental protocol for adsorption

Batch Experiments were conducted in a set of 250ml of flasks containing NPs and nanocomposite films separately and 100ml of both dyes solution separately with varying initial concentrations. The flasks were stirred for 70 minutes at 150 rpm at room temperature until complete decolarization of dye or till equilibrium is not achieved. The adsorption efficiacy of both dyes (Methyl orange and methylene blue) was investigated on T60 UV-VIS Spectrophotometer (PG Instruments UK) by varying concentrations of (1, 3, 5 mg/L), and adsorbent dose (1mg,5mg 10mg) as a function of time. Absorbance of Methyl Orange and Methylene Blue was recorded at respective $\lambda_{max}$ of 465nm and 665nm. Concentration was calculated from standard calibration curve which are mentioned in figure 2.4 and 2.5 respectively while percentage formula was calculated using formual,

$$\% \, R = \frac{Ci - Ct}{Ci} \times 100$$
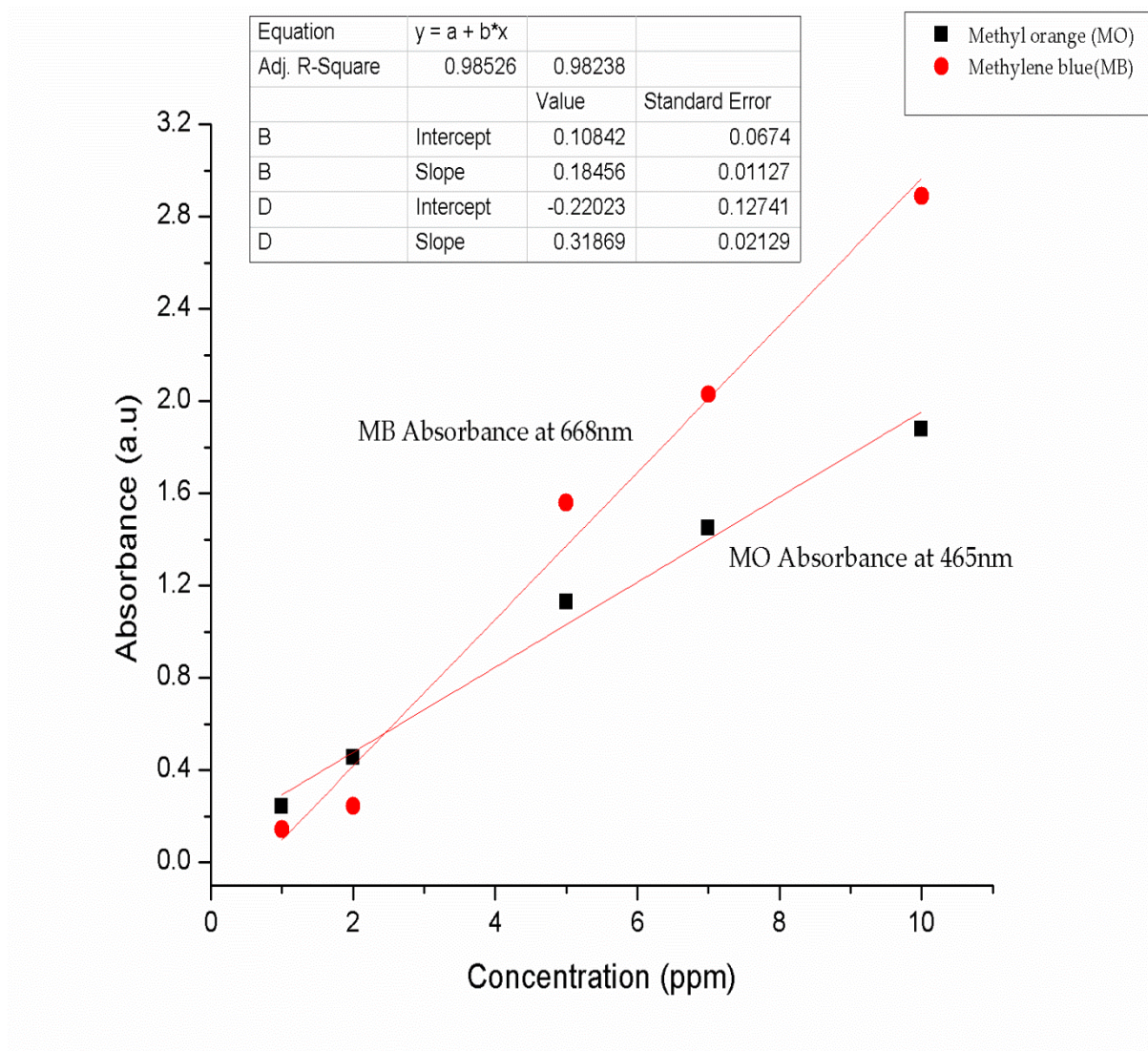
**Figure 2.4 Calibration Curve for Methylene Blue and Methyl Orange**

## 2.10 Equilibrium and Kinetic Studies

Kinetic study was done for calculating adsorption isotherms at different concentrations and mass of adsorbents. Langmuir and Freundilich isotherms were applied at varying conditions for adsorption of azo dyes .

## 2.11 Freundilich Isotherm

Freundilich presented the earliest known sorption isotherm equation (Freundlich, 1906). This model is applicable for sorption on multi layer and heterogeneous surfaces as well [63].

Where $K_F$ is the Freundilich constant and 'n' the Freundilich exponent refers to adsorption capacity or intensity. Slope and intercept is generally obtained by plot of $q_e$ and log $C_e$.

## 2.12 Langmuir isotherm

Quantitatively it describes about the monolayer formation on the exterior surface of adsorbent, [64]. Its linear form can be expressed as,

## 2.13 Adsorption kinetics studies

Kinetic study was performed in order to get insight about the reaction mechanism which is quiet important for determining reaction mechanism and adsorption process efficiency which includes two orders: pseudo first and pseudo second order kinetics.

## 2.14 Pseudo first order kinetics

This rate equation is commonly applied for studying sorption behavior of solute molecules from bulk phase and it is represented as[65].

## 2.15 Pseudo second order kinetics

Second model, which states that adsorption mechanism generally, follows second-order chemi sorption.

## 3.1 Results and Discussion

The present research study comprises of three steps. In first step synthesis of metal nano particles was done from a biosource and preparation of Chitosan /PEG/CuO nano composite films. The second step involves the characterization of synthesized NPs and Chitosan/PEG

films for this they were first of all subjected for FTIR to investigate presence of important functional groups, present in the nano particles which are important for adsorption procedure. The third step of this research study was the adsorption process. Experiments were conducted to evaluate the removal rate of methyl orange and methylene blue dyes on the NPs and adsorbent films at varying parameters.

## 3.2 Adsorbent characterization

Neem Extract and synthesized CuO nano particles were subjected to FTIR analysis to determine the presence of functional groups; their results are summarized in table 3.The IR spectra of all the adsorbents are mentioned in Figure 3 respectively.

## 3.3 FTIR Analysis of CuO NPs and Chitosan/PEG/CuO films

In the IR spectrum of Neem leaf exact, The intense bands occurring at 550 $cm^{-1}$ , 3379 $cm^{-1}$ , 1653.05$cm^{-1}$, 900-1800$cm^{-1}$, 1024.24 $cm^{-1}$, 2962 $cm^{-1}$and 3379 $cm^{-1}$ and 2800-3000 $cm^{-1}$ which corresponds to C-O,O-H stretching's however N-H, C-H, C=O stretching , bending, vibrations were also present which confirms the presence of different organic molecules like

alcohol amines phenol amides amines carboxylic acid group esters in the leaf extract of nee Neem [68] .

The band at 613cm$^{-1}$ indicates the presence of CuO nano particles as reported in the literature [69]. Neem extract contains many phytochemicals such as proteins,, flavonoids,alkaloids here we propose possible mechanism for nanoparticles synthesis at first the metal precursor reacts with (-OH) hydroxyl anions which are produced from water and it forms copper hydroxide. The aqueous extract of Neem leaves contains various phytochemicals these compounds will altogether act as encapsulating agents and reduce copper hydroxide to copper oxide NPs. NPs spectra suggests the presence of different organic molecules due to Neem which was used for its synthesis as described in the previous study [70].
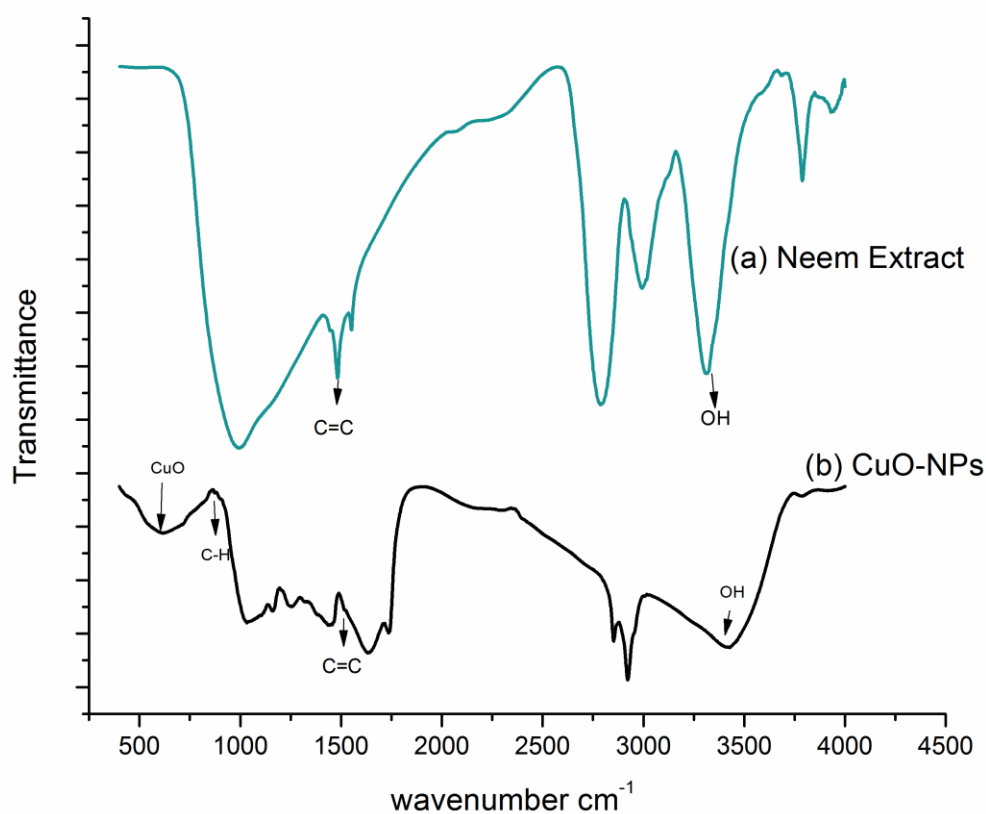


**Figure 3. IR spectra of CuO NPs and Neem Extract**

## 3.4 SEM Analysis of CuO NPs
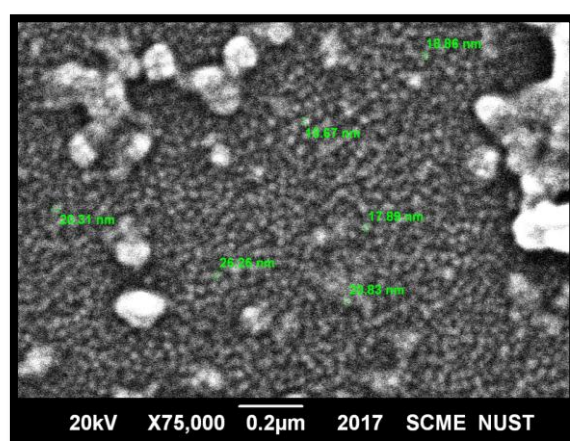


**Figure 3.1 – SEM of CuO NPs**

The morphology of samples surfaces and that of copper oxide NPs were examined by SEM using with current of voltage. Suspension of prepared NPs were Sonicated, further the drop of suspension was used to put on clear dry stubs. Samples were sputtered coated with gold.

The surface morphological features of synthesized nanoparticles were studied by scanning electron microscope. The SEM image figure 3.1 reveals that CuO particles are well dispersed. The appearance of some particles was in spherical shape and some were in oval shape. so the prepared particles were in nanometer range. The average diameters of the particles observed

from SEM were in the range of 16-32 nm. This is very similar to those described in the previous literature [4]. These results indicated that mono-dispersive CuO nanoparticles were obtained [5]. While clusters of NP s can also be observed due to agglomeration .this suggests that NPs have tendency to form clusters due to their high surface energy.

**3.5 X-Ray diffraction of CuO NPs (XRD)**

Different types crystalline phases were identified and determined by means of XRD. Thus, the phases that were present in the synthesized nano particles were studied. Irradiation conditions were 30 and 40mA for the scanning of diffraction angle between 10 and 80.

figure shows noticeable peaks at 35° , 42° , 60° and 75° corresponding to (002) (111) (113) and (004) planes respectively which were in accordance with JCPDS card reference number 01-078-2076.XRD indicates that all the CuO NPs peaks are in well aggreemnet with the standard pattern of monoclinical crystal system. Sharp peaks in the XRD refer to high crystalline nature of the synthesized copper nanoparticles. They also ascribe about the crystallite arrangement which is cubical with (hkl) planes alignment [74]
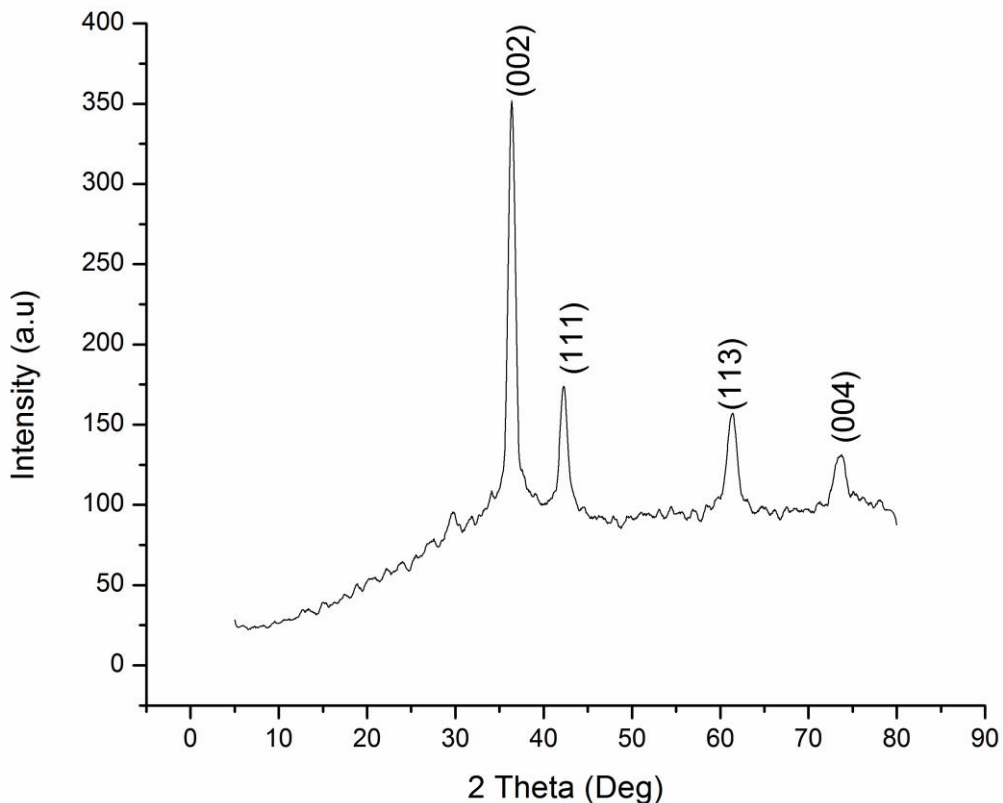


**Figure 3.2 XRD patterns of Copper oxide nano particles**

## 3.6 Attenuated total reflection spectroscopy (ATR) Analysis of Chitosan/PEG/CuO Nano composite films

ATR spectra of nano composite films displayed typical absorption peaks based on composition were present in all the blend interferrograms. pure chitosan shows small peakat 898 cm$^{-1}$ , 1580 cm$^{-1}$ ,1650 cm$^{-1}$,indicates characteristic peak of sacchrides, Amide 1 and Amide II $^{1`}$ while broadening of O-H and N-H groups can be identified around 3400cm$^{-1}$ [75].

Formation of small peaks around 1384.22 cm$^{-1}$ shows the presence of C-O stretching and OH bending vibrations. Intensified peaks around 1098.72 cm$^{-1}$ shows presence of C-N stretching of glycosidic bonds in the pyranose group; indicating polymeric association of Chitosan and PEG while small peaks around 776.38 cm$^{-1}$ corresponds to the C-H rocking ,OH bending and C-C bending. Additional peak at 1750 cm$^{-1}$ was observed which indicates that CuO is bound to the matrix while O-H , N-H Stretching vibrations indicate broad peak in the region of 3006-3500 cm$^{-1}$ [76].

Peak shifting also occurs due to metal co ordination bond between heavy metal and electron rich groups. CuO small peak was present around 613cm$^{-1}$ ATR spectra of blend confirmed the presence of both polymers in blend system [77].
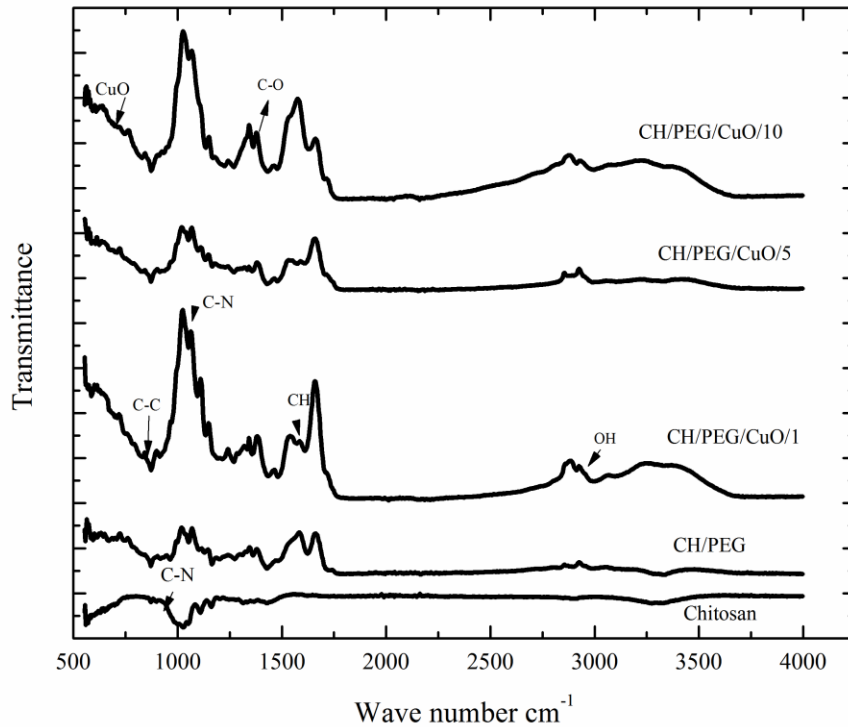
**Figure 3.3 ATR spectra of Nano composite films**

## 3.7 Tensile mechanical properties of pure and Chitosan/PEG/CuO Nano composite films

Tensile properties of pure and blend films were determined using Trapezium testing machine (AG-20KNXD PLUS)

Tensile properties of pure and blend films of Chitosan, PEG and copper oxide nano particles were analyzed. Their stress strain curve is shown in the Figure 3.4respectively,

Tensile properties of pure and blend films contains various filler content which were examined at room temperature. S-S curves of nano composites in figure 3.4 shows the effect of addition of filler in blend system. Tensile properties of pure and composite films are tabulated in table 3.2.
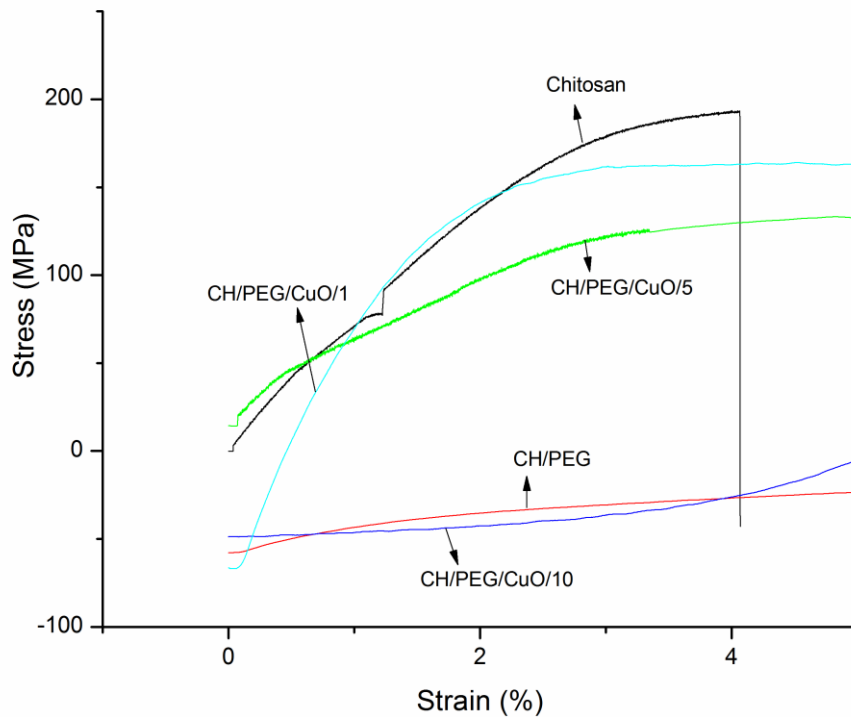
**Figure 3.4 S-S curves of pure and Blend films**

It was observed that by nano filler addition their mechanical strength is enhanced.the enhancement of properties depend solely upon homogeneity, dispersion, orientation of filler material.

Results clearly show that in case of pure films tensile strength was less in comparison to blend films but it gradually increases on addition of nano filler reason could be at highest loading filler and matrix both were compatible with each other and secondary bonding between them was sufficient to support the system. However elongation at break gradually decreases with addition of filler the reason might be the extensive secondary bonding makes the system weaker so the elongation at break decreases [78].
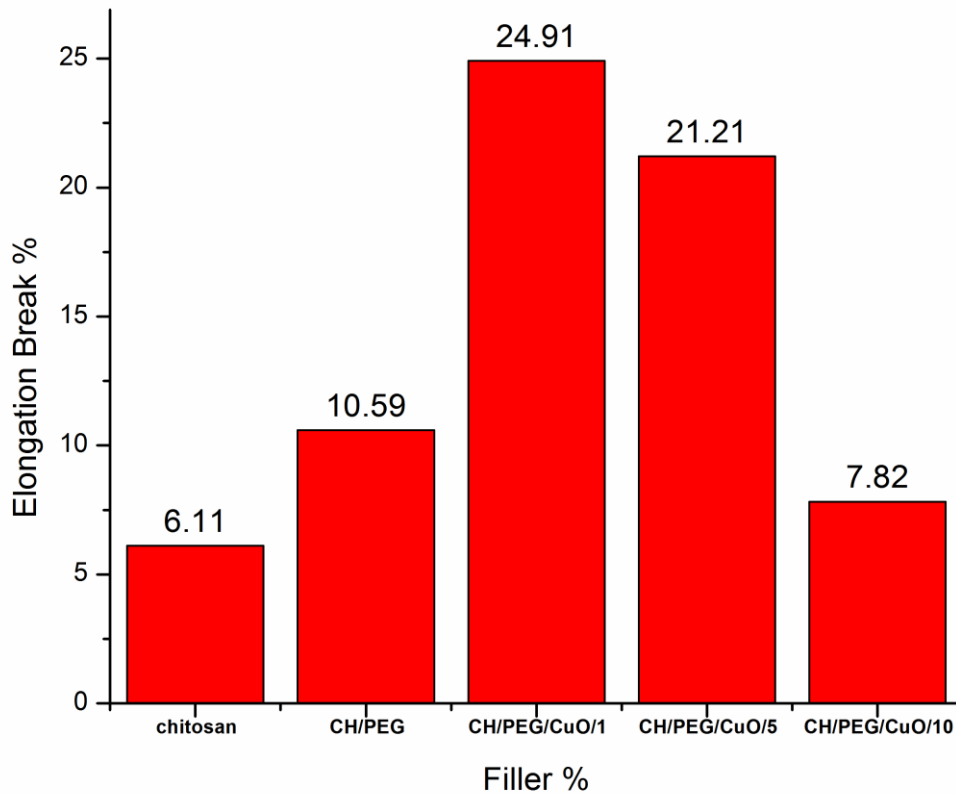
**Figure 3.5 Elongation at break of Blend films**

Highest strength was achieved at 10% loading of nano copper oxide as shown in figure 3.6 whereas tensile strength reaches to maximum which reveals that at this loading percolation reached moreover at such loading ratio distribution, orientation and dispersion; all are properly improved which results in the formation of percolation network, after the percolation network two types of interactions occur; filler-filler and filler matrix , the filler-filler interactions are commonly weaker as compared to filler matrix.
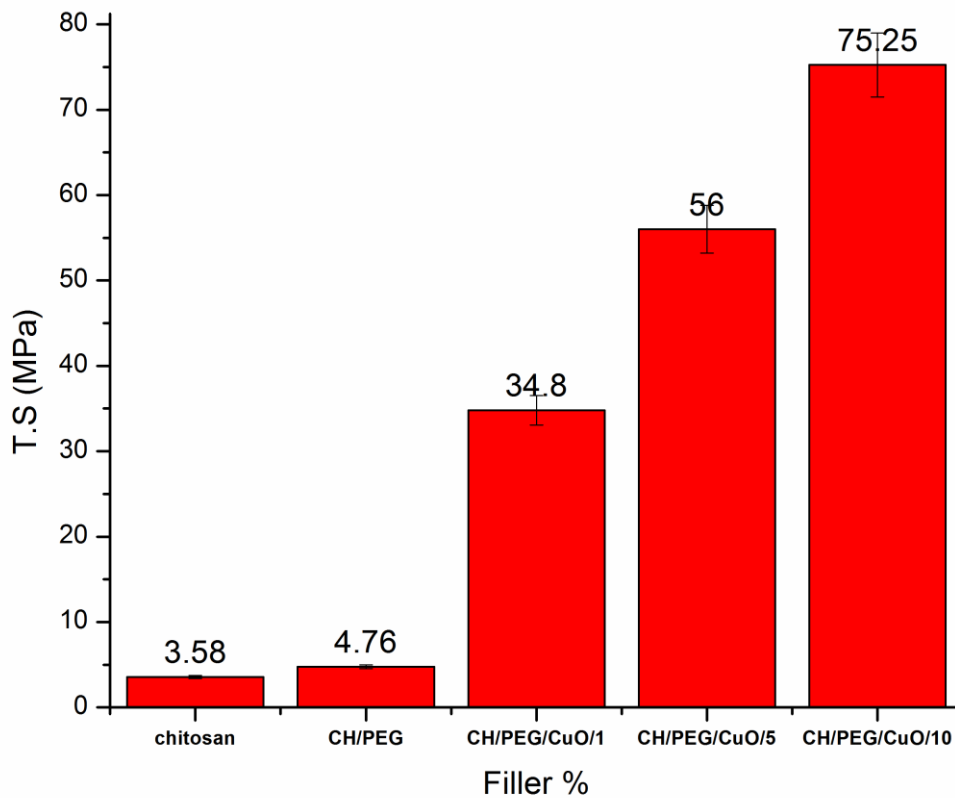
**Figure 3.6 Tensile strength of pure and Blend films**

Tensile moduli is used to measure the stiffness of material the stiffest material has higher moduli

while moduli increases significantly with addition of PEG and copper oxide nano particles as shown in Figure 3.7 the obtained results were 2048MPa at 10% filler loading. At a low filler loading of 1% and 5% respectively. Films show marginal improvement in moduli however better mechanical properties are possible due to strong moleculare interactions between PEG and chitosan which is possible only because of intermolecular hydrogen attractions.
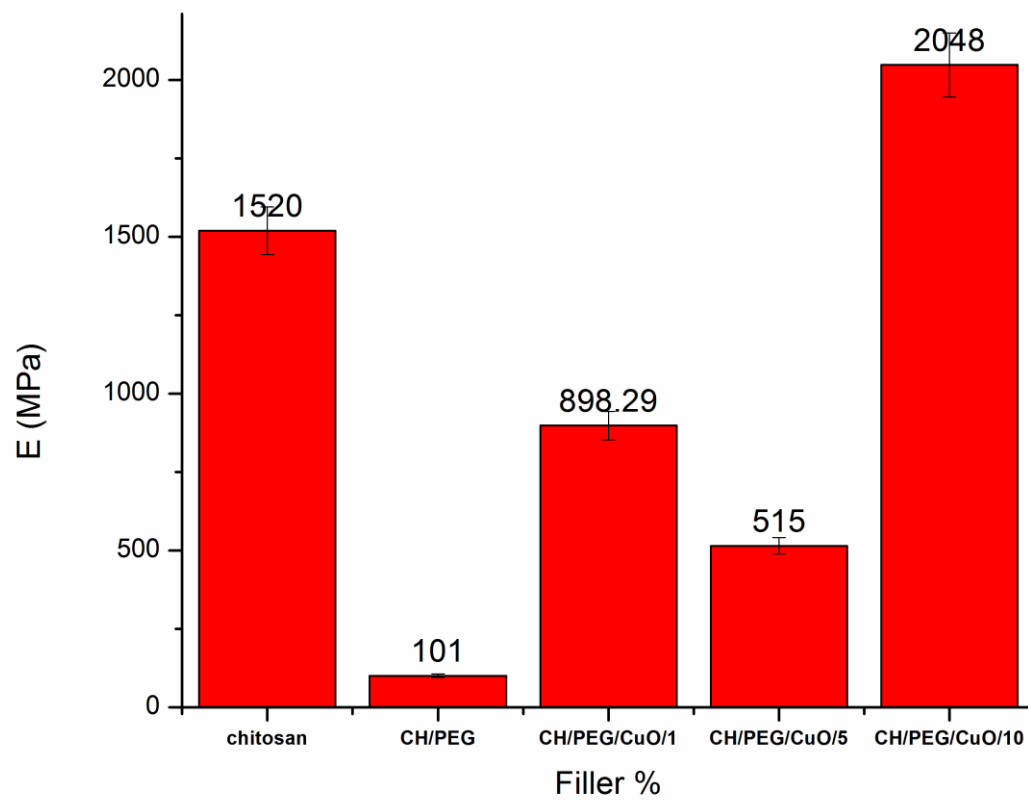
**Figure 3.7 Modulus of Chitosan/PEG/CuO films**

**Table 3.2 Tensile mechanical properties of Chitosan /PEG/CuO films**

| Concentration of filler (mg) | T.S (MPa) | Elongation at break (%) | Modulus (MPa) |
|---|---|---|---|
| Chitosan pure | 3.58 | 6.11 | 1520 |
| CH/PEG | 4.76 | 10.50 | 101 |
| CH/PEG/CuO/1 | 34.8 | 24.91 | 898 |
| CH/PEG/CuO/5 | 56 | 21.21 | 515 |
| CH/PEG/CuO/10 | 75.25 | 7.82 | 2048 |

## 3.8 SEM Analysis of Chitosan/PEG/CuO films

. The morphology of samples surfaces and that of copper oxide NPs are examined by using SEM JEOL-6490A-JSM with current of 41 Ma and 15KV voltage.

Figure 3.9 shows morphological analysis .SEM for topographical analysis of CuO NPs and blend films both were taken for morphological analysis which reveals the microporous surfaces with respect to copper oxide loading in blend films the SEM images figure (a) of pure chitosan film shows no visible pores but a blunt rough surface with cracks while micrographs of CH/PEG film figure (b) shows porous structure with micro voids and cracks. Copper Oxide nano particles loading shows puffy blunt surface with uniform dispersion of nano particles and increased porosity it could be explained on the basis of copper oxide nps agglomeration around polymer chains. Figure 3.9 from (g) to (j) shows cryo structured analysis which reveals the smooth and rough textures  indicating well blending of both matrices and  uniform dispersion of nano particles plus it also confirms that copper oxide nano particles have embedded into blend matrix evenly and uniformly with pores clearly seen in Figure 3.9 (i) and (k)  [79].



10kV    X1,000    10µm    2017   10 50 SEI          20kV    X1,000    10µm    2017   11 50 SEI
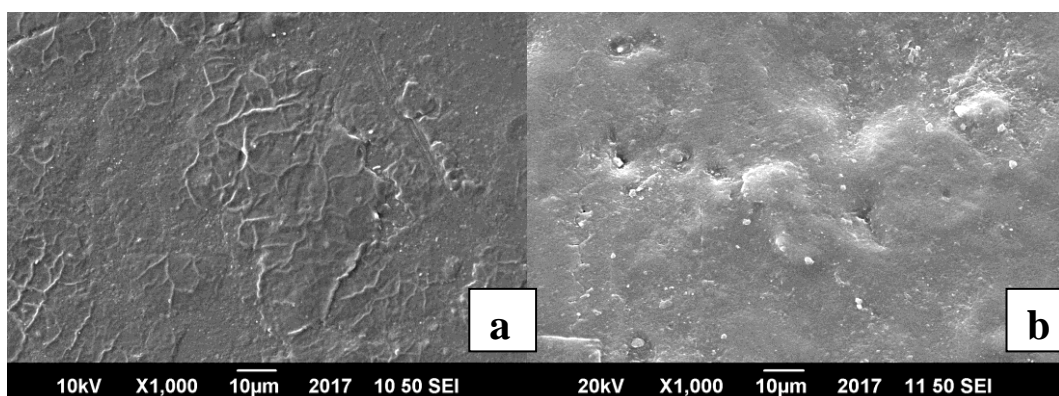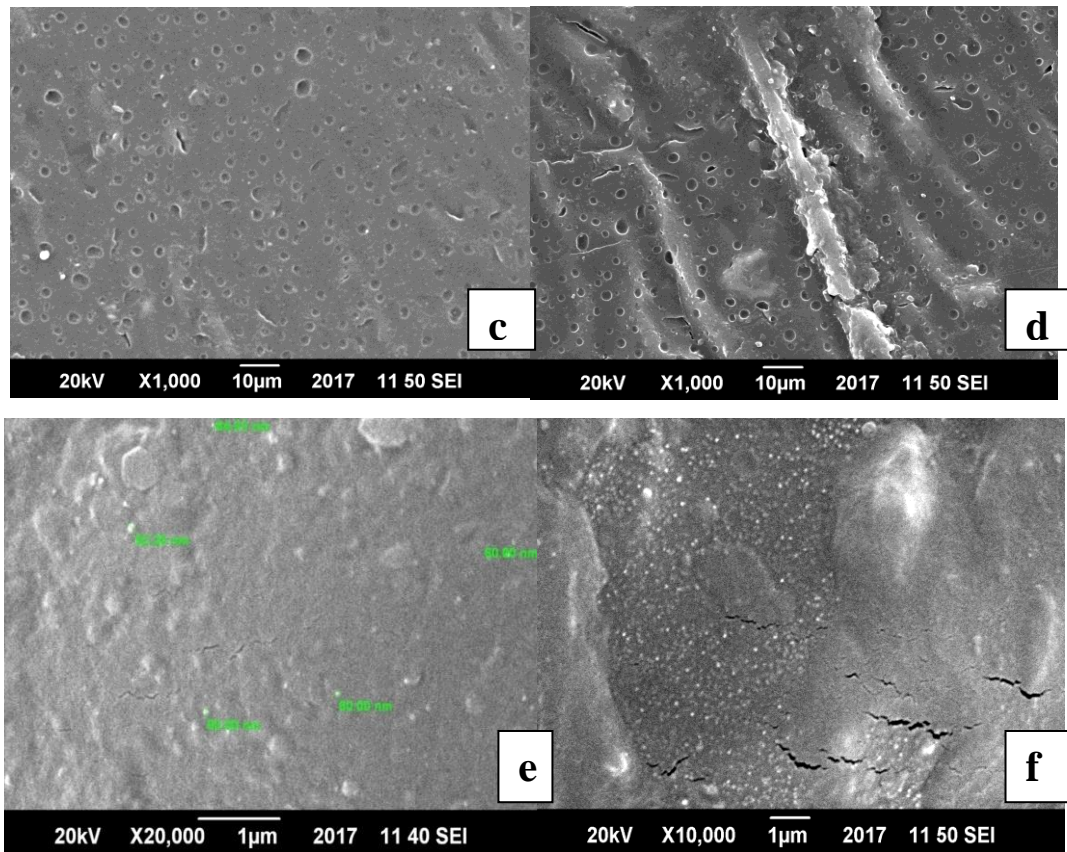
**Figure 3.8 SEM micrographs showing morphology of (a)Pure Chitosan film (b) Blend film (c) Nano composite film at 1mg filler loading (d) Nano composite film at 5mg filler loading (e) Nano composite film at 10mg Filler loading (f) Uniform dispersion of CuO**
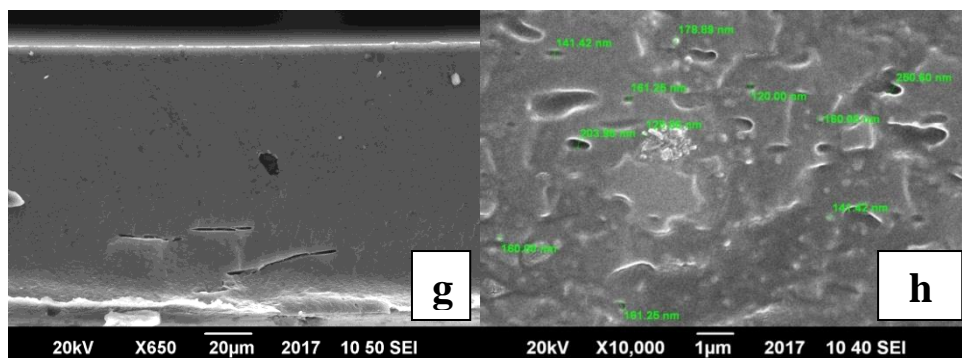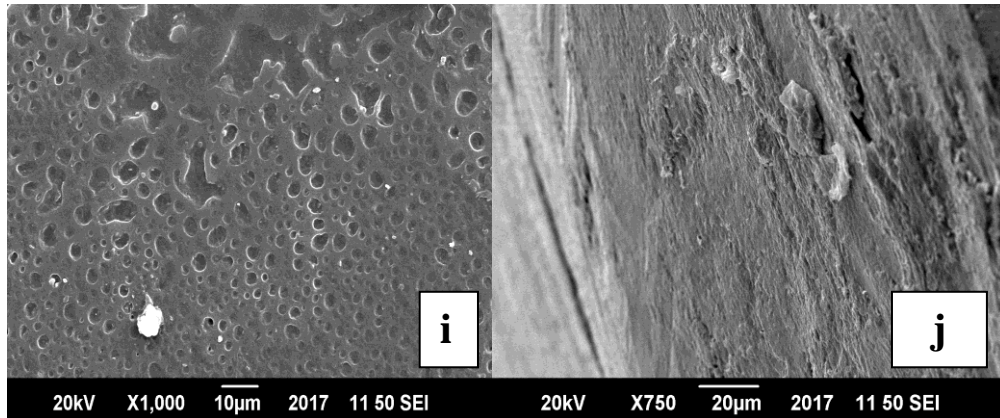
**Figure 3.9 SEM micrographs of cryo structured g) Edge morphology at 1mg Filler loading (h) cross section of Nano composite film (i)Edge morphology at 5mg filler loading (j) Edge morphology at 10mg filler loading**

## 3.9 X-Ray Diffraction analysis of Chitosan/PEG/CuO Films

XRD graph in figure 3.10 confirms the crystalline nature of prepared NPs of copper oxide the identified peaks represent the (hkl) cubic crystal structure.The relatively high intense peak at 45.5° in accordance with other shows the direction of nano crystal growth these results have clearly suggested that copper oxide NPs are successfully synthezied from Neem leaf extract. The broader peaks show size of crystallite to be very small [80].figure 3.10 shows XRD graph of pure and composite films.

The XRD pattern for samples indicate successful deposition of nano particles as prepared samples the graph shows a prominent PEG/CH peak at 2 theta of 25.2 degree. The peak for copper oxide NPs can clearly be seen at 2 theta 35.5 degree referring to (002) plane respectively. Sharp peaks show high crystalline nature of deposited copper oxide NPs, intensity of deposited copper oxide NPs increase with increasing concentration of filler in blend films which also refers to high crystallinity . PEG/CH film shows amorphous nature which refers to good miscibility of films while a shorter hump of characteristic peak at 19.2 degree shows chitosan peak referring to plane (110) [81].

For chitosan seven polymorphs have been proposed which includes "Annealed" "tendon: "L-1" " L-2" forms "1" and "II" and "non crystalline" another study have mentioned three forms "non crystalline" "hydrated crystalline" and "anhydrous crystalline" [82]. the XRD of pure and blend films shown in figure 3.10 gives peak at 2 theta 18.6° , 25.5° assigned to, anhydrous amorphous chitosan structure respectively, while reflection of PEG were at 2

theta 14.5° . The variation of crystalline nature of chitosan could be ascribed to double effect of PEG. PEG addition might weaken the interaction between chitosan and water, thus allows chitosan to crystallize in form of anhydrous structure.

The identified peak shows that samples are composed of copper oxide NPs. PEG/CH being present inside without any other identified impurity therefore it is evident that copper oxide NPs are present in CH/PEG /CuO deposited films samples.
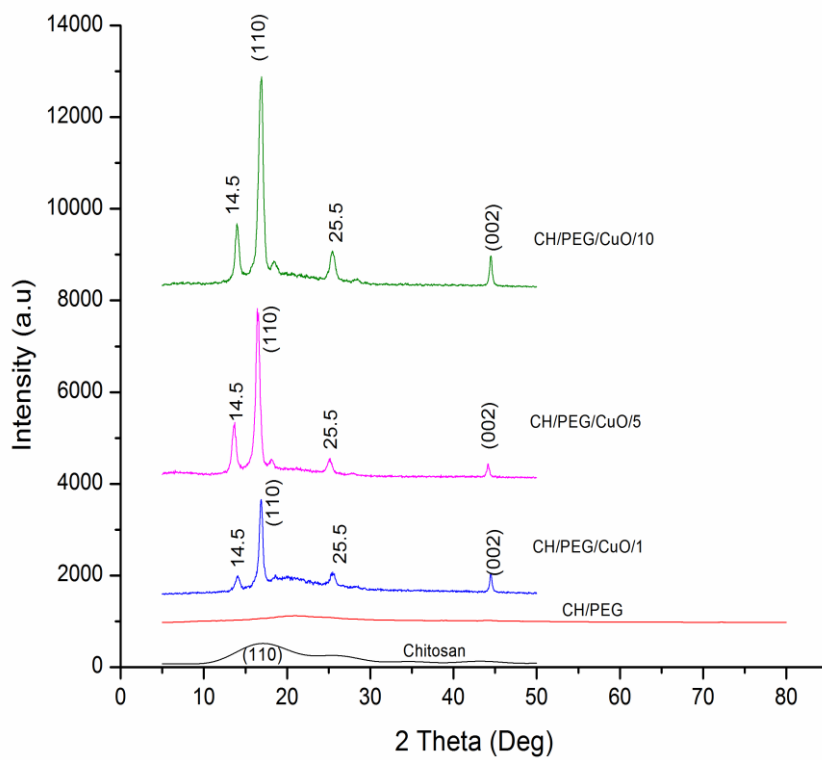


**Figure 3.10 XRD patterns of pure and nano composite films**

## 3.11 Batch adsorption of methyl orange and methylene blue

Batch adsorption experiments were carried out in order to determine the removal efficacy for synthesized blend films as nano sorbents. Different parameters like varying induced concentrations, adsorbent concentration and contact time was studied for each experiment. Acidic and basic (Methyl Orange and Methylene Blue) were selected for present study while adsorbents were synthesized.

# 3.12 Methyl orange and Methylene Blue Dye Adsorption mechanism

The mechanism by which Chitosan helps out in adsorption process has been a matter of concern. different phenomena are involved like, chemisorption, surface adsorption, diffusion, adsorption, complexation however different kind of interactions might also be involved as physical adsorption, vander waals forces, aggregate mechanism and dye-dye interactions etc they all can act together.

 Generally four steps are involved in dye removal process on adsorbent,

1. **Bulk diffusion;** ions migrates from bulk phase tosurface of adsorbent.
2. **Film diffusion ;** dye ions diffuse at surface of adsorbent through boundary layer.
3. **Pore Diffusion;** intra particle diffusion from surface.
4. **Chemical Reaction;** dye molecules get adsorbed at materials active site through chelation, ion exchange, or complexation [85].

**Figure 3.13: Anionic dye adsorption mechanism on Chitosan films [85]**

## 3.13 Batch for removal of Methyl Orange

The synthetic solution of Methyl Orange (acidic) dye was subjected to batch removal using pure,nano composite films and nano particles separately under varying parameters.

## 3.14 Effect of Adsorbent dose

The percentage removal of Methyl Orange was studied by varying the adsorbent dose between 1mg, 5mg and 10mg at a dye concentration of 1mg/L and 5mg/L and 10mg/L. As

shown in Fig.3.14, initially the dye removal increased with the addition of nano filler content as the adsorbent amount of copper oxide and nano filler content in blend films was increased. [85[86]. Incase of blend films Adsorbent concentration of filler at 1mg,5mg,10mg ,Removal efficiency increased upto 94% , such trend can be explained as the availability of more active sites help in further uptake of dye ions .Large pore size of the blend films along with copper oxide nanoparticles play the role in two fold adsorption of dye molecules plus Chitosan molecules also react with the dye molecules via electrostatic interactions and hydrogen bonding Figure 3.14 shows removal efficiency of Pure Chitosan films with less than 10% removal because of its non porous surface which cannot hold dye ions the only factor involved in removal is amine groups attached on Chitosan chains
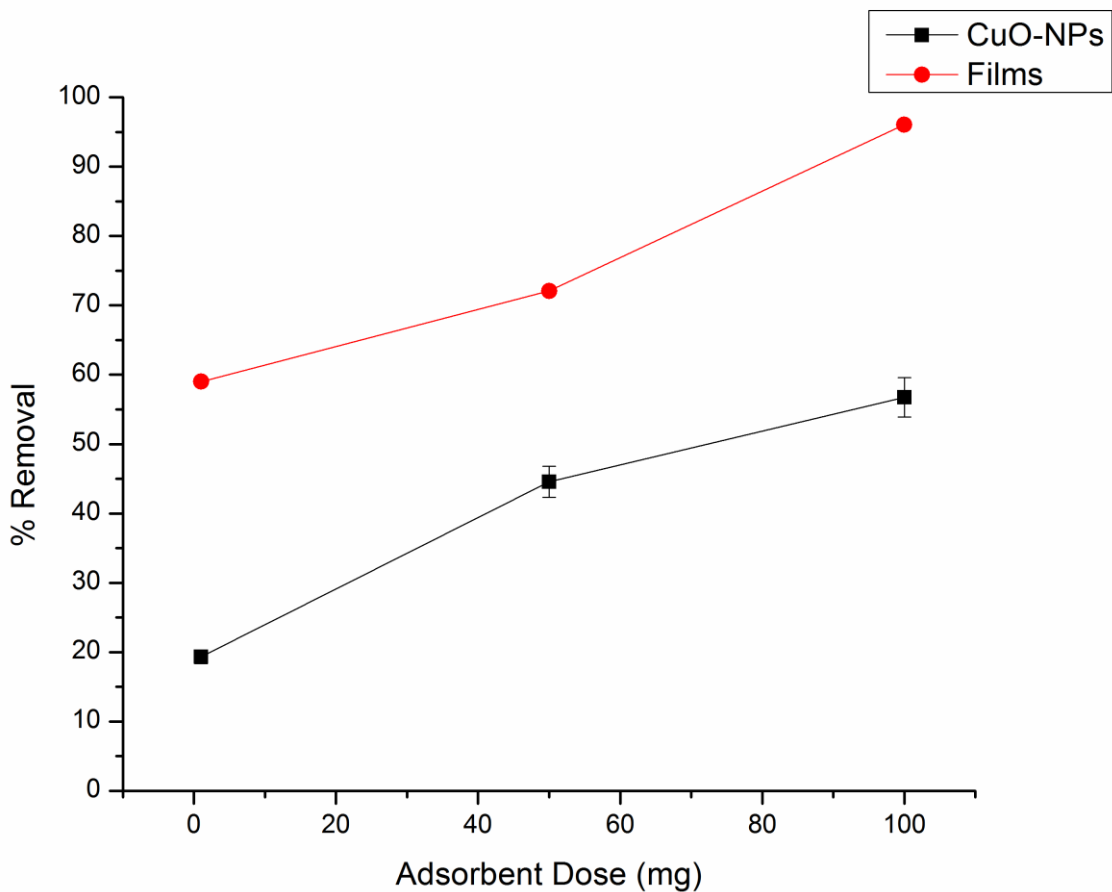


**Figure 3.14:  Percentage Removal Efficiency of Methyl Orange using copper oxide nano particles and Chitosan /PEG/CuO films at varying adsorbents dose of 1,5 and 10mg at optimum 10mg/L of dye.**

## 3.15 Effect of contact time

Figure 3.18 indicates initially the rate of dye removal was fast due to large surfacr area of films which provides more binding sites to the dye molecules [87]. When equilibrium was achieved after 45 minutes time further ptake was stopped due to depletion of active sites.Pure Chitosan films show percentage removal less than 10% reason as shown in figure 3.15 which might be due to non porous surface and the only thing involved in dye uptake was electrostatic attractions between dye molecule and amine groups present in Chitosan.

However for blend films adsorption of dyes was slower initially, and thereafter, it becomes fast near equilibrium. However Contact time presents a fast kinetics or fast forward reaction while equilibrium is achieved after about 50 minutes which indicates the saturation of all active sites [88].
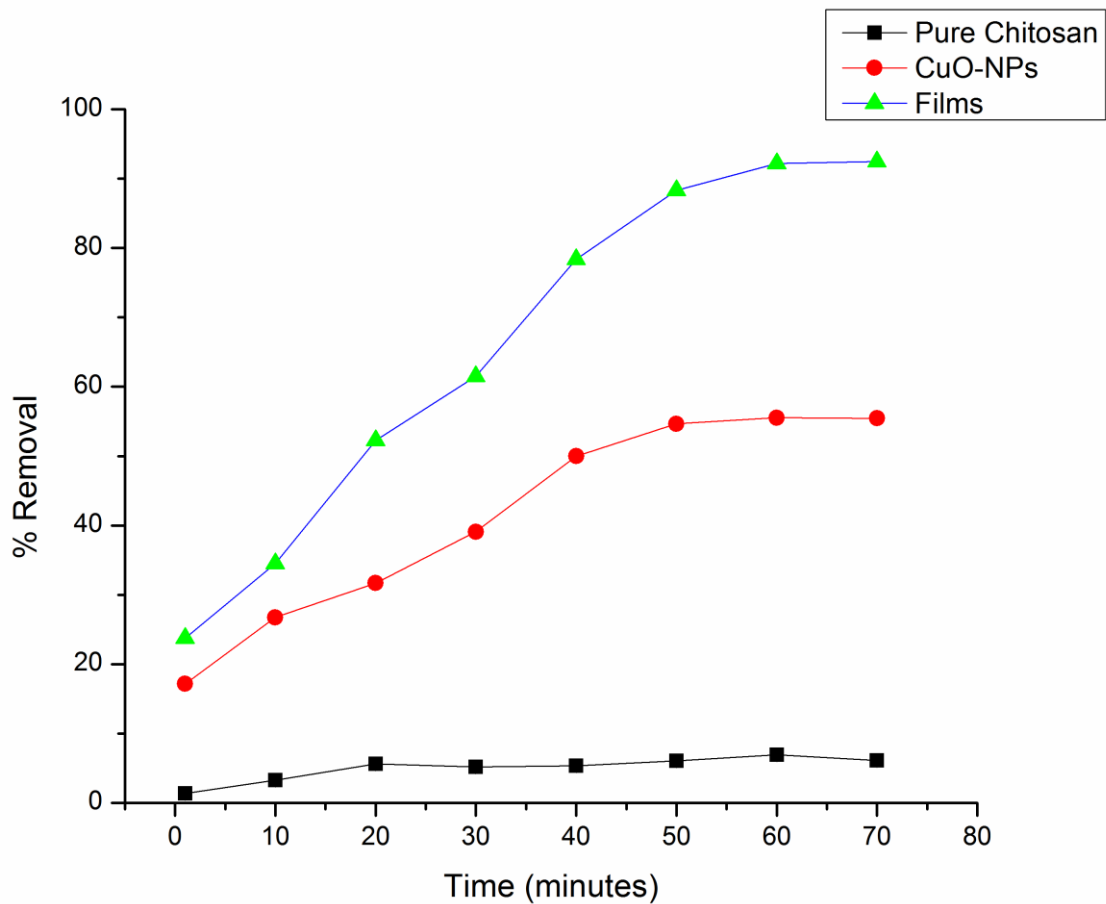


**Figure 3.15: Efficiency of pure Chitosan films , copper oxide nano particles and and Nano Composite films for removal of Methyl Orange at different contact time.**

**Figure 3.16: Types of interactions involved for dye removal [88]**

## 3.16 Effect of initial dye concentration

Adsorption process generally boosts up with the high dye concentration. Maximum dye removal at 10mg/L was achieved (66% and 94% for copper oxide and blend films) respectively at optimum 10mg biosorbents dose [89]. according to figure 3.17  In case of nano particles it was found that an increase in the dye concentration leads to saturation of all the active sites[91].

Agglomeration of nano particles during batch reaction might be the reason for low adsorption which leads to less no of active sites available for dye molecules to adhere. But in case of blend films Electrostatic attractions between the molecules of dye which carry negative charge  and Chitosan/PEG/CuO having positive charge might be the reason for enhanced dye removal [92].
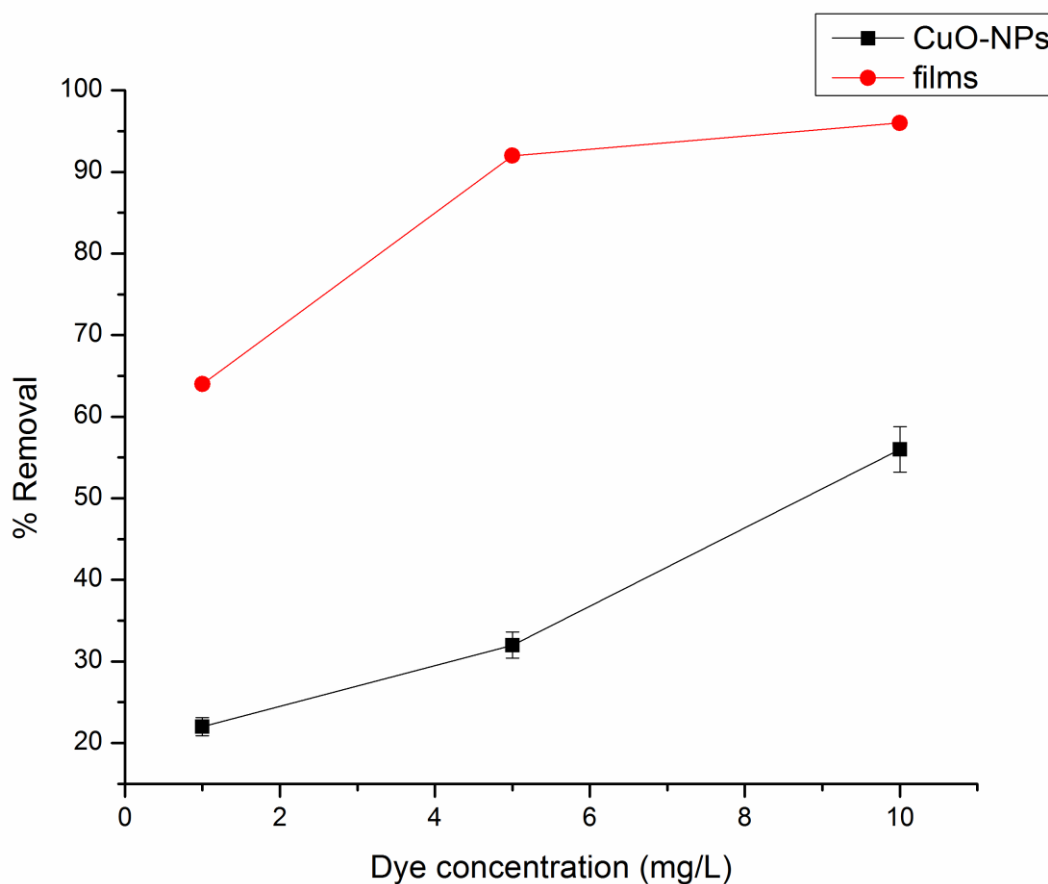
**Figure 3.17: removal percentage for NPs and blend films at varying dye  conc.of 1,5 and 10mg/L at optimum 10mg Dose of Adsorbents.**

## 3.17 Batch for Methylene blue removal

Batches were carried out at different dye concentrations of (1,5 and 10 mg/L) while dose taken was (1mg, 5mg 10mg) in case of copper oxide NPs and Filler concentration of blend films.

**Figure 3.18 structure of Methylene Blue** [95]

## 3.18 Effect of dye conc. on adsorption

Adsorption efficiency of nano adsorbents decreases as dye conc was increased, As it is evident from the figure 3.19, when the dye concentration increased from 1 to 5 mg/L, the percentage removal of dye decreased from 66 to 37% for copper oxide particles. Hence the overall removal percentage decreased, this might be due to agglomeration of adsorbate molecules / overcrowding of active sites or depletion of active sites [93].

In case of Nano composite films dye conc is independent of the dye concentration the larger surface area and electrostatic interactions between adsorbent and dye molecules are the reason for efficient removal [94].
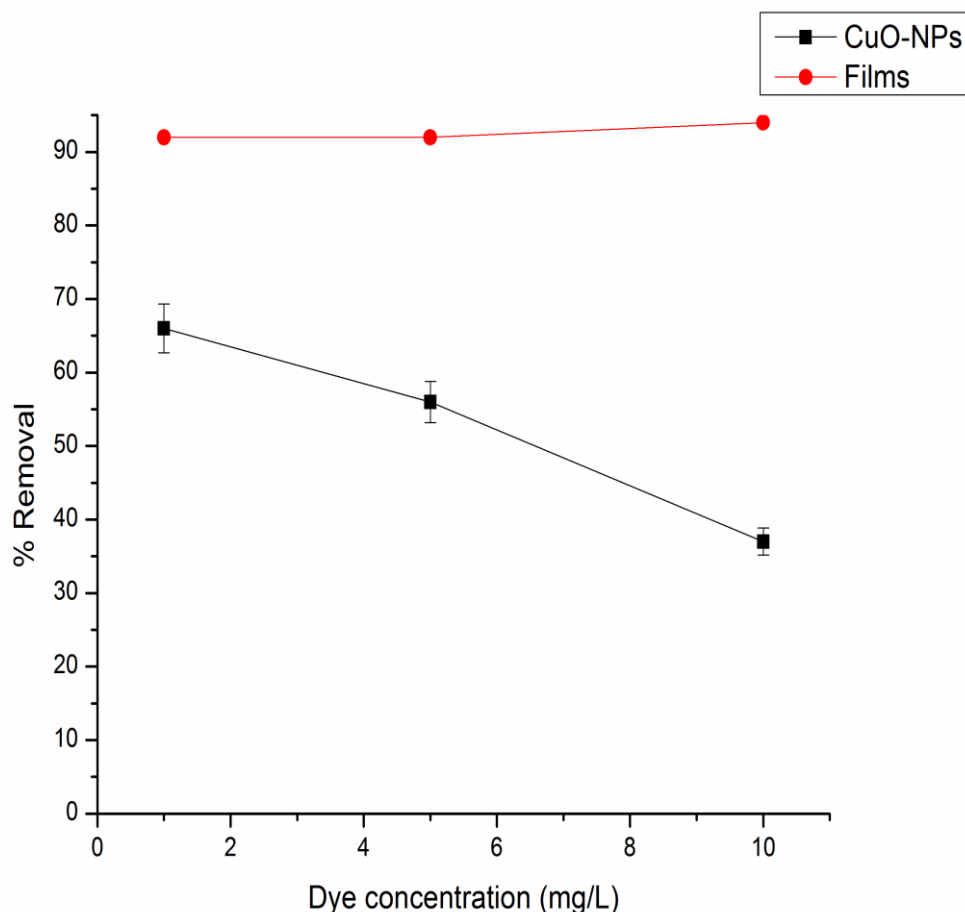
**Figure 3.19: Removal of Methylene Blue using copper oxide nano particles and Nano composite films at different induced concentrations.**

## 3.19 Effect of contact time

Figure 3.21 shows that adsorption occurs very fast initially. Pure chitosan film shows very less removal efficiency and it remains constant till end of reaction time as shown in figure 3.21 reason might be dense structure and brittle nature of Chitosan which retards the overall adsorption while only active part involved is amine groups on surface of Chitosan, while After about 50 minute, the amount of adsorption by CuO particles reaches from 22% to 66 % respectively as shown in figure 3.20. It remains constant afterwards; additionally dye molecules bind to the outer surfaces of adsorbent afterwards it migrates to internal pores and cavities [95].

In figure 3.20 In case of blend films It was observed that adsorption took place on the outside surface as well as inside pores it also suggested that large external surface area due to pores helps in uptaking of small  dye particles as compared to larger particles .initially all the active

sites were unoccupied therefore adsorption was slower in the beginning of reaction but it further proceeds at higher rate when monolayer was formed and all the active sites were occupied completely after reaching equilibrium [96].
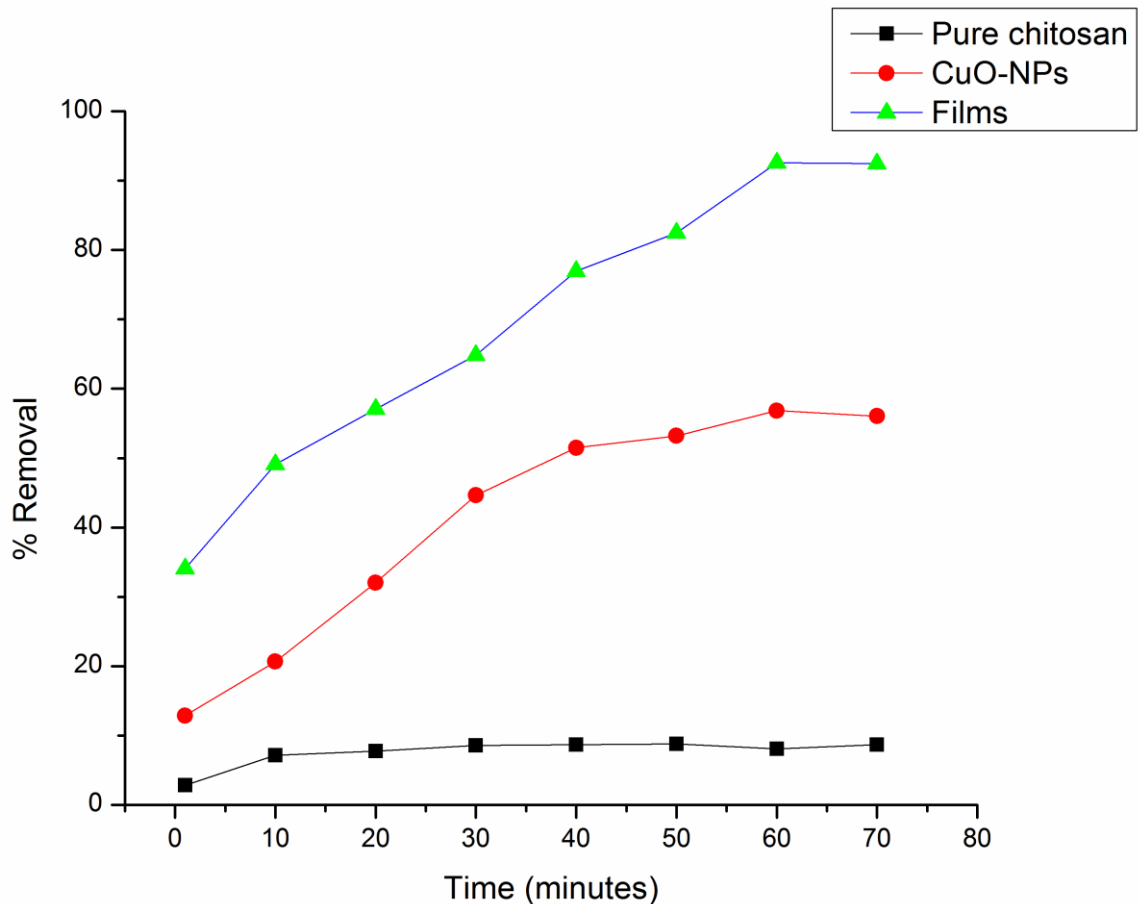


**Figure 3.20: Removal of Methylene Blue using pure Chitosan film, copper oxide nano particles and Nano composite films at different contact time.**

## 3.20 Effect of Adsorbent Dose

Figure 3.21 indicates that by increasing the dose of biosorbent removal efficiency increased significantly. Maximum removal for all nano sorbents was achieved by using 10mg of biosorbent dose with removal efficiency of 66% and 94% for copper oxide nano particles and blend films as shown in figure 3.21 respectively. Such type of trend might be due to presence of more active sites.More the cavities or hollows more the surface area of films would be available so more the uptake of dye molecules [97].
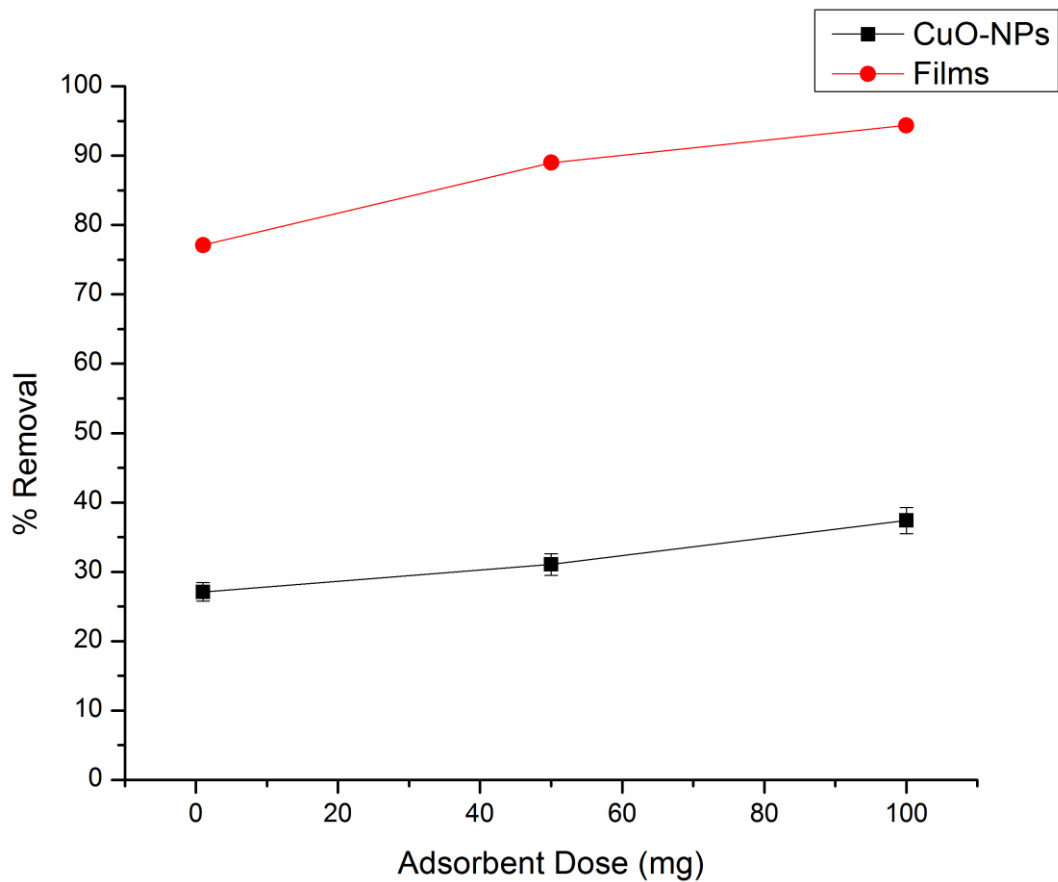
**Figure 3.21: % Removal efficiency of Methylene Blue using Nano composite films and copper oxide nano particles at varying Adsorbent dose and filler concentration .**

## 3.22 Adsorption kinetics and isotherms

The kinetic study aims on investigating the removal capacity in the presence of different parameters like initial concentration, dose and contact time for methyl orange and methylene blue.

Pseudo second order kinetic model
$R^2 = 0.999$
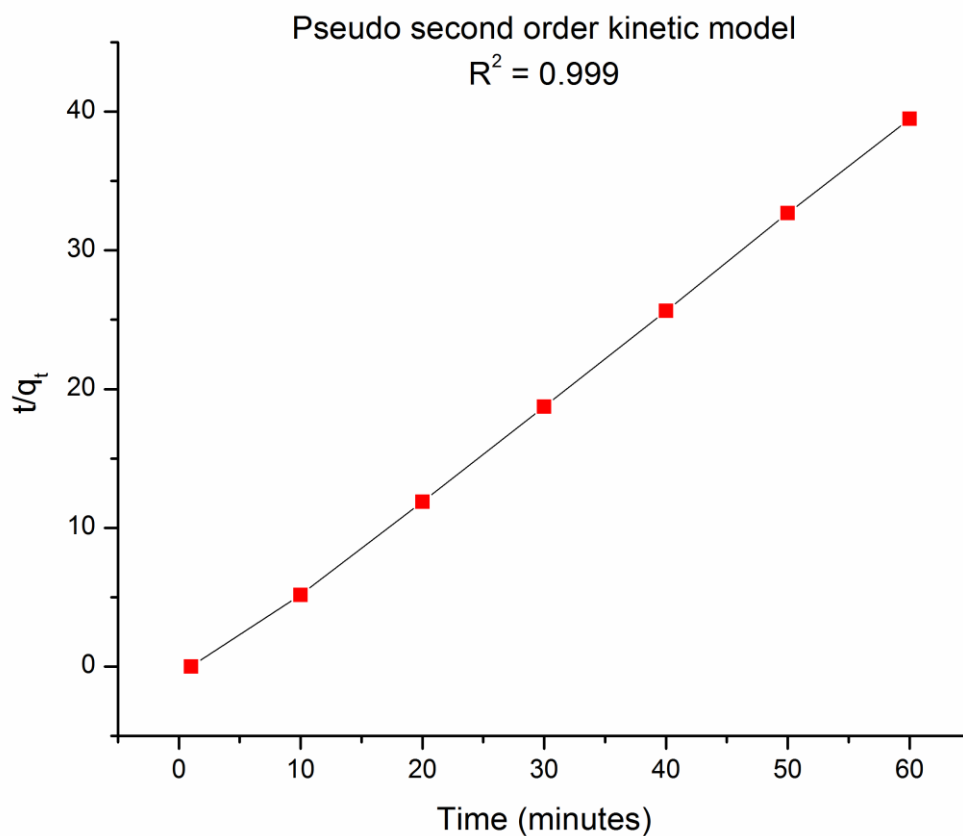
Kinetic data is applied to evaluate the overall removal rate from aqueous phase. to find out the sorption capacity of azo dyes; pseudo first order and pseudo second order were applied. Equilibrium isotherms were used to quantify the adsorptive capacity of adsorbents, for this purpose both isotherms were applied. Results are summarized in table 3.5 and isotherms in figure 3.23.
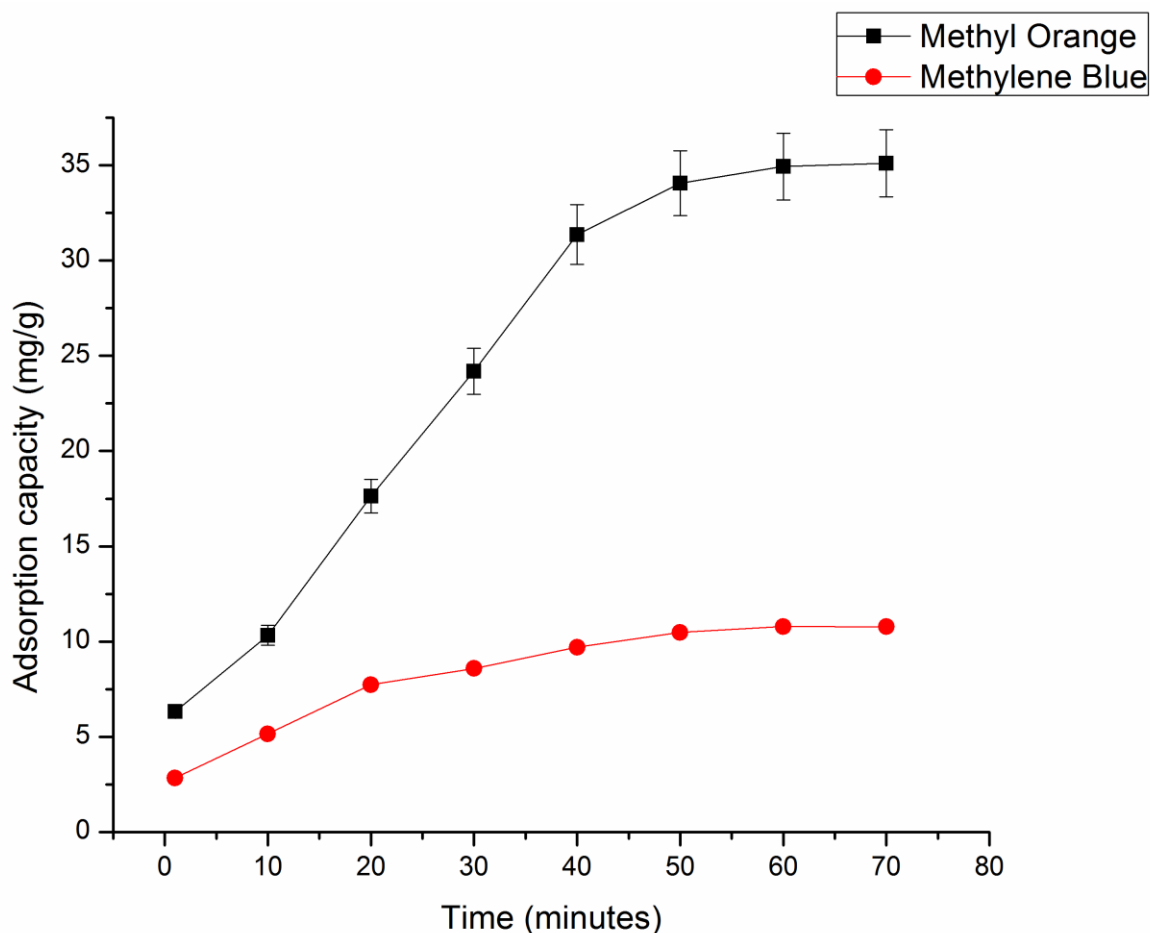
**Figure 3.23 Adsorption isotherms on nanocomposite films**

Results indicate that all adsorbents follow second order which implies to the nature of adsorption which is chemi sorption means chemical interactions took place rather physical bonding. Data also suggests that both models Langmuir and Freundilich were applicable which refers to the fact that mono layer and multi layer sorption took place on surface of nano composite films as well as inside cavities and hollows with adsorption capacity of 35.5 mg/g/min. The value of coefficient for second order kinetics was (0.99) greater than first order of kinetics (0.924) which involves sharing of electrons or their exchange. However the negative value of Langmuir constant for NPs suggest that it gives regression value more than 1 and adsorption of both dyes on synthesized NPs were very difficult.

**Table: 3.6 Adsorption kinetics of Copper oxide nano particles and nano composite films**

| Adsorbents | Adsorption Kinetics | | | | | |
|---|---|---|---|---|---|---|
| | Methyl Orange | | | | | |
| | Pseudo second order | | | First order | | |
| | $K_2$ | $q_e$ | $R^2$ | $K_1$ | $q_e$ | $R^2$ |
| N-Films | 1.337 | 35.5 | 0.998 | 0.014 | 0.875 | 0.674 |
| CuO-NPs | -0.231 | 0.146 | 0.994 | 0.000 | 0.056 | 0.120 |
| | | | | | | |
| Adsorbents | Methylene Blue | | | | | |
| | Pseudo second order | | | First order | | |
| | $K_2$ | $q_e$ | $R^2$ | $K_1$ | $q_e$ | $R^2$ |
| N-Films | 2.661 | 10.83 | 0.952 | 0.012 | 0.371 | 0.924 |
| CuO-NPs | 0.880 | 0.298 | 0.980 | 0.013 | 0.880 | 0.709 |
| | | | | | | |

| Adsorbents | Adsorption isotherm models | | | | | |
|---|---|---|---|---|---|---|
| | Methyl Orange | | | | | |
| | Freundlich isotherm model | | | Langmuir isotherm model | | |
| | $K_F$ | N | $R^2$ | $K_L$ | $Q_m$ | $R^2$ |
| N-Films | 1.343 | 3.121 | 0.999 | 2.219 | 51 | 0.999 |
| CuO-NPs | 10.03 | 9.634 | 0.996 | 1.738 | 0.044 | 1 |
| | | | | | | |
| | Methylene Blue | | | | | |
| | Freundlich isotherm model | | | Langmuir isotherm model | | |
| | $K_F$ | N | $R^2$ | $K_L$ | $Q_m$ | $R^2$ |
| N-Films | 8.231 | 3.822 | 0.958 | 10.73 | 22.38 | 0.894 |
| CuO-NPs | 1.700 | 0.097 | 0.996 | 0.097 | 0.879 | 0.865 |
| | | | | | | |

## Conclusions

The Biosynthesis procedure adopted in this study offer simple, cost effective and efficient procedure for preparation of CuO nano particles of reduced size. FTIR endorsed formation of composites.SEM analysis confirmed the immobilization of NPs onto the composite matrix.XRD results confirm the phase purity and high crystalline nature of filler as well as films.

Synthesis of porous chitosan PEG films loaded with copper oxide as filler shows enhanced mechanical, adsorption and thermal properties. Addition of metallic filler enhanced the overall properties it gives  toughness and strength to the polymer chains.Synthesized nano particles were in nanometer range with reference to SEM results.

The pseudo second order model was more favorable for adsorption of  dyes. Which implies that chemi sorption is the main factor for successful removal of dye For the isotherm studies, both models were applicable i.e.; Freundilich and Langmuir but the best fit isotherm is Freundilich in case of Methylene blue and Langmuir incase of methyl orange respectively. Which refers that multilayer sorption took place as well as monolayer outside the filler surface and inside pores of films.

# References

[1] W. Koros, "Synthetic Polymeric Membranes: A Structural Perspective, By RE Kesting, John Wiley & Sons, 1985, 348 pp," *AIChE Journal,* vol. 33, pp. 171-172, **1987.**

[2] M. Pattanayak and P. Nayak, "Green synthesis and characterization of zero valent iron nanoparticles from the leaf extract of Azadirachta indica (Neem)," *World J. Nano Sci. Technol,* vol. 2, pp. 06-09, **2013**.

[3] N. H. Kalwar, S. T. H. Sherazi, A. R. Khaskheli, K. R. Hallam, T. B. Scott, Z. A. Tagar*, et al.*, "Fabrication of small l-threonine capped nickel nanoparticles and their catalytic application," *Applied Catalysis A: General,* vol. 453, pp. 54-59, **2013**.

[4] H. Chen, J. Wang, D. Huang, X. Chen, J. Zhu, D. Sun*, et al.*, "Plant-mediated synthesis of size-controllable Ni nanoparticles with alfalfa extract," *Materials Letters,* vol. 122, pp. 166-169, **2014**.

[5] M. Asgher, N. Azim, and H. N. Bhatti, "Decolorization of practical textile industry effluents by white rot fungus Coriolus versicolor IBL-04," *Biochemical Engineering Journal,* vol. 47, pp. 61-65, **2009**.

[6] T. G. Chuah, A. Jumasiah, I. Azni, S. Katayon, and S. T. Choong, "Rice husk as a potentially low-cost biosorbent for heavy metal and dye removal: an overview," *Desalination,* vol. 175, pp. 305-316, **2005**.

[7] K. Y. Kumar, H. Muralidhara, Y. A. Nayaka, J. Balasubramanyam, and H. Hanumanthappa, "Low-cost synthesis of metal oxide nanoparticles and their application in adsorption of commercial dye and heavy metal ion in aqueous solution," *Powder technology,* vol. 246, pp. 125-136, **2013**.

[8] S. Iravani, "Green synthesis of metal nanoparticles using plants," *Green Chemistry,* vol. 13, pp. 2638-2650, **2011**.

[9] A. Azizullah, M. N. K. Khattak, P. Richter, and D.-P. Häder, "Water pollution in Pakistan and its impact on public health—a review," *Environment international,* vol. 37, pp. 479-497, **2011**.

[10] Y. Safa and H. N. Bhatti, "Biosorption of Direct Red-31 and Direct Orange-26 dyes by rice husk: Application of factorial design analysis," *Chemical Engineering Research and Design,* vol. 89, pp. 2566-2574, **2011**.

[11] A. K. Verma, R. R. Dash, and P. Bhunia, "A review on chemical coagulation/flocculation technologies for removal of colour from textile wastewaters," *Journal of environmental management,* vol. 93, pp. 154-168, **2012**.

[12] A. K. L. Sajjad, S. Shamaila, B. Tian, F. Chen, and J. Zhang, "Comparative studies of operational parameters of degradation of azo dyes in visible light by highly efficient WOx/TiO2 photocatalyst," *Journal of Hazardous Materials,* vol. 177, pp. 781-791, **2010**.

[13] M. Ahmed, S. Ali, S. El-Dek, and A. Galal, "Magnetite–hematite nanoparticles prepared by green methods for heavy metal ions removal from water," *Materials Science and Engineering: B,* vol. 178, pp. 744-751, **2013**.

[14] Y. Abboud, T. Saffaj, A. Chagraoui, A. El Bouari, K. Brouzi, O. Tanane*, et al.*, "Biosynthesis, characterization and antimicrobial activity of copper oxide nanoparticles (CONPs) produced using brown alga extract (Bifurcaria bifurcata)," *Applied Nanoscience,* vol. 4, pp. 571-576, **2014**.

[15] S. Irem, Q. M. Khan, E. Islam, A. J. Hashmat, M. A. ul Haq, M. Afzal*, et al.*, "Enhanced removal of reactive navy blue dye using powdered orange waste," *Ecological engineering,* vol. 58, pp. 399-405, **2013**.

[16] D. Morshedi, Z. Mohammadi, M. M. A. Boojar, and F. Aliakbari, "Using protein nanofibrils to remove azo dyes from aqueous solution by the coagulation process," *Colloids and Surfaces B: Biointerfaces,* vol. 112, pp. 245-254, **2013**.

[17] H. Tahir, M. Sultan, N. Akhtar, U. Hameed, and T. Abid, "Application of natural and modified sugar cane bagasse for the removal of dye from aqueous solution," *Journal of Saudi Chemical Society,* vol. 20, pp. S115-S121, **2016**.

[18] M. Solís, A. Solís, H. I. Pérez, N. Manjarrez, and M. Flores, "Microbial decolouration of azo dyes: a review," *Process Biochemistry,* vol. 47, pp. 1723-1748, **2012**.

[19] S. Sadaf and H. N. Bhatti, "Batch and fixed bed column studies for the removal of Indosol Yellow BG dye by peanut husk," *Journal of the Taiwan Institute of Chemical Engineers,* vol. 45, pp. 541-553, **2014**.

[20] M. Rafatullah, O. Sulaiman, R. Hashim, and A. Ahmad, "Adsorption of methylene blue on low-cost adsorbents: a review," *Journal of hazardous materials,* vol. 177, pp. 70-80, **2010**.

[21] H. Lachheb, E. Puzenat, A. Houas, M. Ksibi, E. Elaloui, C. Guillard*, et al.*, "Photocatalytic degradation of various types of dyes (Alizarin S, Crocein Orange G,

Methyl Red, Congo Red, Methylene Blue) in water by UV-irradiated titania," *Applied Catalysis B: Environmental,* vol. 39, pp. 75-90, **2002**.

[22]     N. Sriram, D. Reetha, and P. Saranraj, "Biological degradation of Reactive dyes by using bacteria isolated from dye effluent contaminated soil," *Middle–East Journal of Scientific Research,* vol. 17, pp. 1695-1700, **2013**.

[23]     D. Saba Sadiq, A. Yasar, and M. Zakria, "Clean and low cost techniques for textile dye bath effluent treatment."

[24]     N. N. Roselina, A. Azizan, and Z. Lockman, "Synthesis of nickel nanoparticles via non-aqueous polyol method: effect of reaction time," *Sains Malaysiana,* vol. 41, pp. 1037-1042, **2012**.

[25]     T. L. Seey and M. Kassim, "Acidic and basic dyes removal by adsorption on chemically treated mangrove barks," *International Journal of Applied,* vol. 2, pp. 270-276, **2012**.

[26]     N. Mosallanejad and A. Arami, "Kinetics and isotherm of sunset yellow dye adsorption on cadmium sulfide nanoparticle loaded on activated carbon," *Journal of Chemical Health Risks,* vol. 2, **2012**.

[27]     R. Rahimi, H. Kerdari, and M. Rabbani, "Adsorptive removal of crystal violet (CV), a carcinogenic textile dye, from aqueous solution by conducting polyaniline/hollow manganese ferrite nanocomposites," in *ECSOC-14: The 14th International Electronic Conference on Synthetic Organic Chemistry*, **2010**, pp. 1-30.

[28]     H. Khan, N. Ahmad, A. Yasar, and R. Shahid, "Advanced Oxidative Decolorization of Red Cl-5B: Effects of Dye Concentration, Process Optimization and Reaction Kinetics," *Polish journal of environmental studies,* vol. 19, **2010**.

[29]     M. Celebi, M. A. Kaya, M. Altikatoglu, and H. Yildirim, "Removal of cationic dye from textile industry wastewater with using enzyme, fungus and polymer," *TOJSAT,* vol. 3, pp. 39-45, **2013**.

[30]     M. Pattanayak and P. Nayak, "Ecofriendly green synthesis of iron nanoparticles from various plants and spices extract," *International Journal of Plant, Animal and Environmental Sciences,* vol. 3, pp. 68-78, **2013**.

[31]     A. L. Ahmad, W. A. Harris, and B. S. Ooi, "Removal of dye from wastewater of textile industry using membrane technology," *Jurnal Teknologi,* vol. 36, pp. 31-44, **2002**.

[32] R. A. Soomro, S. H. Sherazi, N. Memon, M. Shah, N. Kalwar, K. R. Hallam, *et al.*, "Synthesis of air stable copper nanoparticles and their use in catalysis," *Advanced Materials Letters,* vol. 5, pp. 191-198, **2014**.

[33] M. F. Siddiqui, S. Andleeb, N. Ali, P. B. Ghumro, and S. Ahmed, "Up-flow immobilized fungal Column Reactor for the Treatment of Anthraquinone dye Drimarene blue K sub> 2 RL," *African Journal of Biotechnology,* vol. 8, **2009**.

[34] J. Xiong, Y. Wang, Q. Xue, and X. Wu, "Synthesis of highly stable dispersions of nanosized copper particles using L-ascorbic acid," *Green Chemistry,* vol. 13, pp. 900-904, **2011**.

[35] A. Afkhami and R. Moosavi, "Adsorptive removal of Congo red, a carcinogenic textile dye, from aqueous solutions by maghemite nanoparticles," *Journal of Hazardous Materials,* vol. 174, pp. 398-403, **2010**.

[36] S. R. Khalighi, N. M. Khosravi, K. Badii, and L. N. Yousefi, "Adsorption of Acid Blue 92 dye on modified diatomite by nickel oxide nanoparticles in aqueous solutions," **2012**.

[37] B. Padhi, "Pollution due to synthetic dyes toxicity & carcinogenicity studies and remediation," *International Journal of Environmental Sciences,* vol. 3, p. 940, **2012**.

[38] N. Febriana, S. O. Lesmana, F. E. Soetaredjo, J. Sunarso, and S. Ismadji, "Neem leaf utilization for copper ions removal from aqueous solution," *Journal of the Taiwan Institute of Chemical Engineers,* vol. 41, pp. 111-114, **2010**.

[39] Y.-H. Shih, C.-P. Tso, and L.-Y. Tung, "Rapid degradation of methyl orange with nanoscale zerovalent iron particles," *Nanotechnology,* vol. 7, p. 7, **2010**.

[40] I. Prabha I. Prabha and S. Lathasree S. Lathasree, *Photocatalytic Degradation Efficiency of Nanoparticle For The Degradation of Azo Dye in Wastewater Effluents* vol. 4, **2011**.

[41] N. N. Nassar and A. Ringsred, "Rapid adsorption of methylene blue from aqueous solutions by goethite nanoadsorbents," *Environmental Engineering Science,* vol. 29, pp. 790-797, **2012**.

[42] S. Hyder and A. Bari, "Characterization and study of correlations among major pollution parameters in textile wastewater," *Mehran University Research Journal of Engineering and Technology,* vol. 30, pp. 577-582, **2011**.

[43] U. Rafique, A. Imtiaz, and A. K. Khan, "Synthesis, characterization and application of nanomaterials for the removal of emerging pollutants from industrial waste water,

kinetics and equilibrium model," *Journal of Water Sustainability,* vol. 2, pp. 233-244, **2012**.

[44]    C. Song, S. Wu, M. Cheng, P. Tao, M. Shao, and G. Gao, "Adsorption studies of coconut shell carbons prepared by KOH activation for removal of lead (II) from aqueous solutions," *Sustainability,* vol. 6, pp. 86-98, **2014**.

[45]    D. Iqbal, S. Ahmed, D. Alam, and D. Ahmed, "Sustainable management of textile waste water of Pakistan," *World Water Day April,* pp. 96-105, **2011**.

[46]    R. Sankar, P. Manikandan, V. Malarvizhi, T. Fathima, K. S. Shivashangari, and V. Ravikumar, "Green synthesis of colloidal copper oxide nanoparticles using Carica papaya and its application in photocatalytic dye degradation," *Spectrochimica Acta Part A: Molecular and Biomolecular Spectroscopy,* vol. 121, pp. 746-750, **2014.**

[47]    O. V. Kharissova, H. R. Dias, B. I. Kharisov, B. O. Pérez, and V. M. J. Pérez, "The greener synthesis of nanoparticles," *Trends in biotechnology,* vol. 31, pp. 240-248, **2013**.

[48]    L.-h. He, R. Xue, D.-b. Yang, Y. Liu, and R. Song, "Effects of blending chitosan with PEG on surface morphology, crystallization and thermal properties," *Chinese Journal of Polymer Science,* vol. 27, pp. 501-510, **2009**.

[49]    A. Martínez-Camacho, M. Cortez-Rocha, J. Ezquerra-Brauer, A. Graciano-Verdugo, F. Rodriguez-Félix, M. Castillo-Ortega*, et al.*, "Chitosan composite films: Thermal, structural, mechanical and antifungal properties," *Carbohydrate Polymers,* vol. 82, pp. 305-315, **2010**.

[50]    G. Sun, X.-Z. Zhang, and C.-C. Chu, "Effect of the molecular weight of polyethylene glycol (PEG) on the properties of chitosan-PEG-poly (N-isopropylacrylamide) hydrogels," *Journal of Materials Science: Materials in Medicine,* vol. 19, pp. 2865-2872, **2008**.

[51]    Q. Wang, Z. Dong, Y. Du, and J. F. Kennedy, "Controlled release of ciprofloxacin hydrochloride from chitosan/polyethylene glycol blend films," *Carbohydrate polymers,* vol. 69, pp. 336-343, **2007**.

[52]    C. Pillai, W. Paul, and C. P. Sharma, "Chitin and chitosan polymers: Chemistry, solubility and fiber formation," *Progress in polymer science,* vol. 34, pp. 641-678, **2009**.

[53]    Y. Liu and H.-I. Kim, "Characterization and antibacterial properties of genipin-crosslinked chitosan/poly (ethylene glycol)/ZnO/Ag nanocomposites," *Carbohydrate polymers,* vol. 89, pp. 111-116, **2012**.

[54] A. E.-A. A. Said, A. A. M. Aly, M. N. Goda, M. Abd El-Aal, and M. Abdelazim, "Modified Sugarcane Bagasse with Tartaric Acid for Removal of Diazonium Blue from Aqueous Solutions," *Journal of Polymers and the Environment,* vol. 26, pp. 2424-2433, **2018**.

[55] M. N. V. Ravi Kumar, "A review of chitin and chitosan applications," *Reactive and Functional Polymers,* vol. 46, pp. 1-27, **2000**.

[56] P. K. Dutta, M. Ravikumar, and J. Dutta, "Chitin and chitosan for versatile applications," *Journal of Macromolecular Science, Part C: Polymer Reviews,* vol. 42, pp. 307-354, **2002**.

[57] S. K. Mishra, D. S. Mary, and S. Kannan, "Copper incorporated microporous chitosan-polyethylene glycol hydrogels loaded with naproxen for effective drug release and anti-infection wound dressing," *International journal of biological macromolecules,* vol. 95, pp. 928-937, **2017**.

[58] A. Y. Ghidan, T. M. Al-Antary, and A. M. Awwad, "Green synthesis of copper oxide nanoparticles using Punica granatum peels extract: effect on green peach Aphid," *Environmental Nanotechnology, Monitoring & Management,* vol. 6, pp. 95-98, **2016.**

[59] D. Rehana, D. Mahendiran, R. S. Kumar, and A. K. Rahiman, "Evaluation of antioxidant and anticancer activity of copper oxide nanoparticles synthesized using medicinally important plant extracts," *Biomedicine & Pharmacotherapy,* vol. 89, pp. 1067-1077, **2017**.

[60] P. Kolhe and R. M. Kannan, "Improvement in ductility of chitosan through blending and copolymerization with PEG: FTIR investigation of molecular interactions," *Biomacromolecules,* vol. 4, pp. 173-180, **2003**.